



# 1 **Reconstructing the ocean's mesopelagic zone** 2 **carbon budget: sensitivity and estimation of** 3 **parameters associated with prokaryotic** 4 **remineralization**

5 Chloé Baumas<sup>1\*#</sup>, Robin Fuchs<sup>1,2\*</sup>, Marc Garel<sup>1</sup>, Jean-Christophe Poggiale<sup>1</sup>, Laurent Memery<sup>3</sup>,  
6 Frédéric A.C. Le Moigne<sup>1,3</sup>, Christian Tamburini<sup>1</sup>

7 *\*Both authors contributed equally*

8 <sup>1</sup>Aix Marseille Univ, Université de Toulon, CNRS, IRD, MIO UM 110, Marseille, France

9 <sup>2</sup>Aix Marseille Univ, CNRS, I2M, Marseille, France

10 <sup>3</sup>LEMAR Laboratoire des Sciences de l'Environnement Marin, UMR6539, CNRS, UBO, IFREMER, IRD, Plouzané,  
11 Technopôle Brest-Iroise, France

12  
13 #Corresponding author : chloe.baumas@mio.osupytheas.fr

## 14 **Abstract**

15 Through the constant rain of sinking marine particles in the ocean, carbon (C) trapped within  
16 is exported into the water column and sequestered when reaching depths below the  
17 mesopelagic zone. Atmospheric CO<sub>2</sub> levels are thereby strongly related to the magnitude of  
18 carbon export fluxes in the mesopelagic zone. Sinking particles represent the main source of  
19 carbon and energy for mesopelagic organisms, attenuating the C export flux along the water  
20 column. Attempts to quantify the amount of C exported versus consumed by heterotrophic  
21 organisms have increased in recent decades. Yet, most of the conducted estimations have led  
22 to estimated C demands several times higher than the measured C export fluxes. The choice  
23 of parameters such as growth efficiencies or various conversion factors is known to greatly  
24 impact the resulting C budget. In parallel, field or experimental data are sorely lacking to  
25 obtain accurate values of these crucial overlooked parameters. In this study, we identify the  
26 most influential of these parameters and perform inversion of a mechanistic model. Further,  
27 we determine the optimal parameter values as the ones that best explain the observed  
28 prokaryotic respiration, the prokaryotic production, and the zooplankton respirations. The  
29 consistency of the resulting C-budget suggests that such budgets can be adequately balanced  
30 when using appropriate parameters.



31 **Keywords:** Biological carbon pump, Optimization methods, Carbon budget, Mesopelagic  
32 zone, prokaryotic carbon demand, model inversion  
33  
34

## 35 1. Introduction

36 The biological carbon pump (BCP) is the main mechanism by which CO<sub>2</sub> is exported and stored  
37 in the deep ocean in the long term. This ecosystem service is defined as the sum of the  
38 biological processes that lead to carbon export from the euphotic zone into the deep ocean  
39 (Eppley and Peterson 1979). This process exports from 5 to 20 Gt C yr<sup>-1</sup> in the form of  
40 particulate organic carbon (POC) gravitationally sinking from the sunlit ocean to the  
41 mesopelagic zone roughly located between 200 and 1000 m (Henson et al. 2011). Therefore,  
42 atmospheric CO<sub>2</sub> levels are strongly related to any change in carbon export into the  
43 mesopelagic zone (Kwon et al. 2009). Five downward pathways of organic matter export to  
44 the mesopelagic zone are defined: through phytoplankton (senescent cells, colonies, spores,  
45 cysts), zooplankton (carcasses or fecal pellets), aggregates (marine snow of different  
46 compositions including the two latter categories), vertical migration of zooplankton and  
47 mixing/diffusion/advection (Siegel et al. 2016; Le Moigne 2019).

48 Gravitational sinking POC supply, known as the dominant pathway, constitutes the main  
49 organic carbon input to the mesopelagic zone (Boyd et al. 2019). Consequently, the downward  
50 flux of organic carbon is attenuated with increasing depth as it is fragmented, metabolized and  
51 remineralized by different biological processes until only the refractory material remains. The  
52 majority of POC flux attenuation occurs in the mesopelagic zone (Martin et al. 1987; Marsay  
53 et al. 2015; Fuchs et al. 2022). The remineralization of exported carbon is mainly performed  
54 by two types of organisms: micro-organisms (mostly heterotrophic prokaryotes i.e. Bacteria  
55 and Archaea) and zooplankton. Heterotrophic prokaryotes primarily use dissolved organic  
56 carbon (DOC) as a source of carbon. However, some prokaryotes, colonizing particles upon  
57 formation, undergo changes in environmental conditions during their descent, such as the  
58 increase of the hydrostatic pressure and the variations of temperature (Tamburini et al. 2003,  
59 2021; Baumas et al. 2021). Such particle-attached prokaryotes primarily use POC as a carbon  
60 source. Only organic matter of size below 600 Da diffuses directly through prokaryotic  
61 membranes, therefore attached prokaryotes produce ectoenzymes required to solubilize larger  
62 molecules (Weiss et al. 1991). Smith et al. (1992) observed that the amount of DOC produced  
63 by ecto-enzymatic solubilization of POC may be 10 to 100 times greater than the absorption  
64 capacity of a cell. DOC is thereby released into the surrounding water (the so-called



65 solubilization). This increases the amount of DOC available for free-living prokaryotes. In  
66 addition, several types of zooplankton are involved in marine particles: POC-feeding  
67 detritivores (e.g. copepods), prokaryotes consumers (e.g. flagellates), and carnivores (e.g.  
68 chaetognaths). Besides, zooplankton lose POC through excretion (moult, mucilage, urine),  
69 fecal pellets (decomposed organic matter), and sloppy feeding. Giering et al. (2014) specify  
70 that 30% of a particle supplied by the downward flux is fragmented by the action of the  
71 detritivores and is transformed into suspended matter.

72 Given their importance regarding the BCP, all the processes described above were extensively  
73 studied in the last decades (e.g. Alldredge and Silver 1988; Smith et al. 1992; Kiørboe et al.  
74 2002, 2003; Kiørboe 2003; Lampitt et al. 2008; Steinberg et al. 2008; Iversen et al. 2010;  
75 Giering et al. 2014; Koski et al. 2020 and references therein). However, the scientific  
76 community has struggled to reconcile the mesopelagic carbon budget with measurements and  
77 estimates showing a biological carbon demand often greater than the amount of known organic  
78 carbon sources (Reinthal et al. 2006; Steinberg et al. 2008; Burd et al. 2010; Collins et al.  
79 2015; Boyd et al. 2019). In other words, the measured export flux cannot sustain measured  
80 metabolic demands of prokaryotes and zooplankton altogether in the mesopelagic zone, leading  
81 to a discrepancy in C budgets.

82 A first explanation may lie in the choices of the boundaries of the mesopelagic zone used to  
83 integrate fluxes and to estimate the carbon budget as investigated in Fuchs et al. (2022). Indeed  
84 they specifically designed a method to determine from CTD-cast variables (fluorescence, O<sub>2</sub>  
85 concentration, potential temperature, salinity, and density) accurate boundaries. With their  
86 method named RUBALIZ, they show that 90% of the POC flux attenuation occurs within new  
87 determined boundaries which is not the case of the fixed 200-1000m often used. Besides,  
88 integrating prokaryotic C demand within RUBALIZ boundaries helps to reduce the  
89 discrepancy. Other response elements may be found focusing on the carbon demand of  
90 prokaryotes (which are responsible for the final step of the remineralization), whose estimation  
91 is usually provided by adding rates of prokaryotic heterotrophic production (PHP) to that of  
92 prokaryotic respiration (PR) (Burd et al. 2010). PHP rates are often measured from tritiated  
93 leucine incorporation rates in incubations which are then multiplied by a conversion factor  
94 Leu/Carbon (CF) (Kirchman et al. 1985). The PR is more challenging to measure (especially  
95 in the dark ocean, (Nagata et al. 2010)) and, therefore, often estimated from measurements of  
96 PHP and a prokaryotic growth efficiency (PGE) taken from the literature (as  $PR = PHP \times (1 - PGE)$ /  
97 PGE), del Giorgio and Cole 1998). Unfortunately, *in-situ* measurements of both CF and



98 PGE are time-consuming and operationally complex to perform (especially for the mesopelagic  
99 zone). In addition, such data for attached to sinking particles prokaryotic communities are  
100 scarce since the adequate sampling devices (to specifically sample biologically intact sinking  
101 particles) were only recently validated (Baumas et al. 2021). Besides, PHP and PR data are  
102 usually obtained after decompression or carried out from experiments at atmospheric pressure,  
103 being a source of misvaluation (Tamburini et al. 2013). As a result, values from the mean of  
104 global literature compilation or theoretical values are often used as references for both CF or  
105 PGE (Burd et al. 2010; Giering and Evans 2022) and may be far from the actual *in situ* values.

106 In parallel, model predictions help to estimate unmeasurable processes along with the  
107 comparison and validation of data. The biological processes occurring in the mesopelagic zone  
108 are not yet well constrained (see sections above). Consequently, only a few models specifically  
109 designed to assess the fluxes governing the BCP in the mesopelagic zone exist (e.g. Tian et al.  
110 2000; Anderson and Ryabchenko 2009; Anderson and Tang 2010; Fennel et al. 2022). For  
111 instance, the model developed by Anderson and Tang (2010) enables the evaluation of the  
112 remineralization of different compartments such as attached prokaryotes to sinking and  
113 suspended particles, free-living prokaryotes and up to six trophic levels of zooplankton. This  
114 model describes the various known biological processes involved in the BCP system. However,  
115 the model also requires to be set up with parameters such as the PGE. For example, Anderson's  
116 model requires 24 parameters which often present large uncertainties.

117 Giering et al. (2014) attempted to reconcile carbon input and biological carbon demand in the  
118 mesopelagic zone using the Anderson and Tang (2010) model and measurements carried out  
119 in the North Atlantic (Porcupine Abyssal Plain site, 49.0°N 16.5°W, summer 2009). They  
120 found that prokaryotes were responsible for 70-92% of the remineralization of organic carbon.  
121 In this study, the model results were consistent with the measurements performed *in situ*, both  
122 showing a reconciliation of the carbon budget between 50 and 1000 m depths. Giering et al.  
123 (2014) balanced their C-budget by using a rather low CF ( $CF = 0.44 \text{ kg C mol}^{-1}$ ) compared to  
124 the one generally used in the literature ( $CF = 1.55 \text{ kg C mol}^{-1}$ ) and a PGE of 8% for free-living  
125 prokaryotes and 24% for prokaryotes attached to the particles. All these values were chosen as  
126 medians of literature values compiled from various measurement methods. Wisely choosing  
127 these parameter is therefore crucial to determine the reconciliation or the imbalance of carbon  
128 budget.

129 In this respect, we rely on model inversion methods (Tarantola 2005) to provide meaningful  
130 estimations of parameters of interest. For a given phenomenon, inversion methods rely on a



131 model taking as input the parameters to be estimated and whose outputs can be compared with  
132 *in situ* measurements. The inversion procedure thus gives the value of the parameters that best  
133 replicate the *in situ* measurements. This type of procedure has already been used in  
134 oceanography modeling. For instance, Saint-Béat et al. (2018) studied phytoplankton marine  
135 food web in the Arctic and Saint-Béat et al. (2020) examined pelagic ecosystems of two  
136 different zones in the Arctic Baffin Bay using inversion method and sensitivity analyses to  
137 identify which biological processes impact the most the planktonic ecosystem functioning.

138 Here, we investigate the impact of overlooked but widely used parameters associated with the  
139 prokaryotic remineralization (e.g. CF, PGEs) on the magnitude of the discrepancy. Our aims  
140 are: 1) to highlight the most sensitive parameters for which the determination of an accurate  
141 value is critical in the context of balancing of mesopelagic carbon budget; 2) to perform a  
142 mathematical inversion method to estimate the most plausible *in situ* values of the most  
143 sensitive parameters from a limited field dataset; 3) to discuss our results in the context of  
144 mesopelagic carbon budget and carbon sequestration by the BCP.

## 145 **2. Material & methods**

### 146 **2.1 *In situ* Data**

147 Most of the data used in this study originated from the DY032 (June-July 2015) cruise at the  
148 PAP (Porcupine Abyssal Plain) site in the North Atlantic onboard the RRS Discovery. Some  
149 data unavailable for DY032 were estimated from a previous PAP cruise, D341 (July-August  
150 2009). Most of the *in situ* data were compiled from already published cruise data (e.g. Giering  
151 et al. 2014; Belcher et al. 2016; Baumas et al. 2021; Fuchs et al. 2022). Their post-treatments  
152 to suit our study framework are described below. Additionally, we used data (ecto-enzymatic  
153 activities along with total hydrolysable amino acids and carbohydrates, depth profile of  
154 heterotrophic prokaryotic production and respiration under *in situ* pressure versus atmospheric)  
155 from the PEACETIME cruise (Guieu et al. 2020) that occurred in May 2017 in the  
156 Mediterranean Sea to illustrate some points in our discussions (see supp data).

#### 157 **2.1.1 Carbon fluxes**

##### 158 **a) Determination of the Active Mesopelagic zone boundaries**

159 Fuchs et al. (2022) introduced the “RUBALIZ” method, using CTD data, which allows the  
160 estimation of vertical boundaries targeting the zone of the dark ocean where most of the POC



161 fluxes attenuation occurs. At station PAP during cruise DY032, this so-called “Active  
162 Mesopelagic Zone” was located between 127 and 751 m.

### 163 **b) Carbon inputs**

164 The POC inputs to the active mesopelagic zone mainly involve the gravitational export of POC.  
165 Gravitational input was taken from Fuchs et al. (2022) who fitted a power law Martin curve (b  
166 of 0.84) on data obtained from 30 to 500m using Marine Snow Catcher (Belcher et al. 2016).  
167 However, gravitational input is not the only POC input known in the literature. Recently, Boyd  
168 et al. (2019), provided an estimation of other particle-injection pumps (PIPs) such as the mixed  
169 layer pump, physical pump, the seasonal lipid pump or the active transport related to metazoans  
170 migrations. At the PAP site during summer, only the eddy subduction pump, metazoans  
171 migrations, and large-scale physical pumps were relevant to take into account. Other PIPs do  
172 not correspond to the location and season considered in our study. From Boyd et al. (2019)  
173 review, these three particle-injection pumps seem to represent altogether around 52% of the  
174 gravitational export of POC. We therefore add up this proportion of POC to the purely  
175 gravitational inputs. This yields an overall POC flux of  $134 \text{ mg C m}^{-2} \text{ d}^{-1}$  exported into the  
176 active mesopelagic zone. The corresponding net POC input is  $117 \text{ mg C m}^{-2} \text{ d}^{-1}$  (that is POC  
177 fluxes at the end - 751 m - of the active mesopelagic zone subtracted to the one at the start -  
178 127 m - for PAP DY032).

179 DOC inputs are taken from Giering et al. (2014) and are considered as the sum of direct DOC  
180 export via physical processes (advection-diffusion) and active flux from zooplankton  
181 migrations. We estimated from their extended Data Fig. 2 that the DOC gradient below 100m  
182 is hardly visible meaning that physical vertical DOC export is insignificant for the active  
183 mesopelagic zone which is studied here. As a result, we set the DOC export at  $3 \text{ mg C m}^{-2} \text{ d}^{-1}$ ,  
184 which corresponds only to the active flux from zooplankton migrations from Giering et al.  
185 (2014).

### 186 **c) Carbon demands**

187 As explained above, prokaryotic carbon demand is generally assessed by adding rates of  
188 prokaryotic heterotrophic production (PHP) to that of prokaryotic respiration (PR). PHP of  
189 non-sinking prokaryotes (that is free-living and attached to suspended particles prokaryotes)  
190 are derived from leucine incorporation measurements on seawater samples and are taken from  
191 Fuchs et al. (2022). These data did not permit the separation of the free-living from attached to  
192 suspended particles (Baumas et al. 2021). Hence, in the sequel, we no longer make this



193 distinction and group both types under the term “non-sinking prokaryotes”. During DY032,  
194 Marine Snow Catchers (MSC) were deployed to separate slow and fast-sinking particles from  
195 100L of samples (Riley et al. 2012; Baumas et al. 2021). PHP rates associated with prokaryotic  
196 communities of fast-sinking particles were taken from Baumas et al. (2021) and slow-sinking  
197 particles are presented here. Briefly, slow-sinking particle fractions were sampled in the 7L  
198 base of the MSC. Samples were incubated and leucine incorporation rates were measured as  
199 for fast-sinking particles in Baumas et al. (2021). The formula described in Baumas et al. (2021)  
200 was then applied to normalize to 100L as particles were concentrated in 7L after 2h of  
201 decantation and to remove the contribution of non-sinking prokaryotes which were primarily  
202 in this compartment around slow-sinking particles of interest. Total sinking prokaryotes PHP  
203 rates were obtained by adding both fast-sinking and slow-sinking prokaryotes PHP rates. In  
204 addition, we were able to use the respiration rates of prokaryotes attached to fast-sinking  
205 particles obtained by Belcher et al. (2016). For each depth (30-500m) the mean total O<sub>2</sub>  
206 consumption per particle in nmol agg<sup>-1</sup>d<sup>-1</sup> was converted to mg C m<sup>-3</sup> d<sup>-1</sup> (assuming a respiration  
207 quotient RQ(CO<sub>2</sub>/O<sub>2</sub>) = 1) by multiplying by the total number of particles (i.e. fecal pellets +  
208 phytoplanktonic aggregates) and dividing by 95L which is the volume of the MSC used (Riley  
209 et al. 2012). It is also important to note that PR for slow-sinking particles is missing. Thus,  
210 when we mention the respiration of sinking prokaryotes, only attached to fast-sinking  
211 prokaryotes are taken into account which certainly underestimates the respiration used. All  
212 prokaryotic carbon demand (PHPs and PRs) estimates were integrated within RUBALIZ  
213 boundaries (i.e. 127m - 751m). Non-sinking prokaryotes PHP rates were integrated using a  
214 piecewise model with a single node on the log-data as described in Fuchs et al. (2022). Sinking  
215 prokaryotes PHP rates were integrated using power law. Sinking PR were integrated using  
216 trapeze because data are only available until 500m and without any *a priori* on the curve shape,  
217 this method is certainly the most conservative.

218 Zooplankton activities are known to be related to POC concentration (Steinberg et al. 2008).  
219 Zooplankton respiration data were available only for the cruise D341 when the net POC input  
220 into the active mesopelagic layer was 59 mg C m<sup>-2</sup> d<sup>-1</sup> (including PIPs) instead of 134 mg C m<sup>-2</sup>  
221 d<sup>-1</sup> for DY032 (see above). For D341, zooplankton respiration integrated within the active  
222 mesopelagic zone (135-726m, Fuchs et al. 2022) was 9 mg C m<sup>-2</sup> d<sup>-1</sup>. Zooplankton respiration  
223 was integrated using a power law as in Giering et al. (2014). Zooplankton respiration data are  
224 missing for DY032, thus we consider this quantity as a percentage of the POC input that we  
225 calculate from the D341 data set, i.e. 14.67%. The zooplankton respiration value used here is  
226 therefore 17 mg C m<sup>-2</sup> d<sup>-1</sup>.



227 *Table 1: Fluxes and their associated values used in this study. Anderson & Tang model's terms*  
 228 *(Anderson and Tang 2010) corresponding to these fluxes are also shown. Values are integrated*  
 229 *between 127 and 751m which are boundaries of the active mesopelagic zone defined by Fuchs*  
 230 *et al. (2022). POC and DOC refer respectively to Particulate and Dissolved Organic Carbon,*  
 231 *PHP to Prokaryotic Heterotrophic Production, and PR to Prokaryotic Respiration.*

Name	Anderson and Tang's Model term correspondence	Values	units	sources
Net POC input	$DI_{ex}$	117	mg C m <sup>-2</sup> d <sup>-1</sup>	Belcher et al. (2016); Boyd et al. (2019)
DOC input	$DOC_{ex}$	3	mg C m <sup>-2</sup> d <sup>-1</sup>	Giering et al. (2014)
Non-sinking prokaryotes PHP	$F_{BFL} + F_{BAD2}$	1.10E+07	pmol Leu m <sup>-2</sup> d <sup>-1</sup>	Baumas et al. (2021)
Sinking prokaryotes PHP	$F_{BAD1}$	1.02E+06	pmol Leu m <sup>-2</sup> d <sup>-1</sup>	Baumas et al. (2021)
Sinking prokaryotes PR	$R_{BAD1}$	19	mg C m <sup>-2</sup> d <sup>-1</sup>	Adapted from Belcher et al. (2016)
Zooplankton respiration	$R_{VA} + R_{VFL} + R_H + R_{Z1:6}$	17	mg C m <sup>-2</sup> d <sup>-1</sup>	Adapted from Giering et al. (2014)

232

## 233 2.2 Mathematical methods

### 234 2.2.1 Parameter estimation

235 The scope of our study is to estimate *in situ* parameters by inverting the model introduced by  
 236 Anderson and Tang (2010), adapted by Giering et al. (2014). We do not intend to present the  
 237 model in details here. The details of the equations constituting the version of the model used  
 238 can be found in the original paper (Anderson and Tang 2010), in the R code available at  
 239 <https://github.com/RobeeF/InverseCarbonBudgetEstim> and the specific terms related to  
 240 [variables used are reported in Table 1](#). The model is calibrated by choosing the set of input





241 parameters that yields the best fit between the model output and the data. As the model outputs  
242 85 outfluxes, we used a subset of four measurable outfluxes to calibrate the model: the PHP of  
243 non-sinking prokaryotes, the PHP of sinking prokaryotes, the PR of sinking prokaryotes and  
244 the respiration of zooplankton. These fluxes have been chosen because of their near direct  
245 correspondence with outputs of the model linked to the C demand of all groups (sinking  
246 prokaryotes, non-sinking prokaryotes, detritivores, bacterivores, and carnivores).

247 Similarly, the model relies on 24 input parameters (Table S1), which makes the parameter  
248 space of significant size and therefore challenging to explore. As such, we first determine the  
249 set of parameters that have the largest impact on the output of the model. Then for these  
250 parameters, the values that give the best fit between the data and the solution given by the  
251 model are determined.

#### 252 a) Sensitivity of the model to its inputs

253 In order to reduce the size of the input parameter space, Sobol Indices (Sobol 1993) were used  
254 to determine the most influential parameters. These indices enable quantification of the share  
255 of the variation of the output that can be imputed to each input parameter.

256 In essence, the first-order Sobol indices account for the direct influence of an input variable on  
257 the output. However, first-order Sobol indices neglect the interactions existing between this  
258 input variable and the other input variables. As such, in addition to the first-order Sobol Indices,  
259 we used the total Sobol indices introduced by Homma and Saltelli (1996) which encompass  
260 both the direct effect of a parameter and also its interactions with the other parameters.

261 First-order and total Sobol indices were computed to quantify the influence of each parameter  
262 over each of the four outfluxes. Only the parameters which had significant Sobol indices (i.e.  
263 Sobol indices > 0.20) for at least one outflux were kept.

#### 264 b) Estimation of the parameters

265 The parameters which had no substantial effects on the output of the model were set to the  
266 values indicated by Anderson and Tang (2010) and Giering et al. (2014) and given in Appendix  
267 (Table S1). The other parameters were estimated by minimizing the distance existing between  
268 the four outfluxes predicted by the model and their *in situ* measured counterpart. The distance  
269 chosen here is a standardized Euclidean distance:



270

$$271 \quad \sum_{i=1}^4 \left( \frac{\text{outflux}_{\text{obs},i} - \text{outflux}_{\text{model},i}}{\text{outflux}_{\text{obs},i}} \right)^2 \quad (1)$$

272 where  $\text{outflux}_{\text{obs},i}$  is the  $i$ -th measured flux and  $\text{outflux}_{\text{model},i}$  its modeled counterpart. The  
273 optimization method used is the Nelder-Mead algorithm (Nelder and Mead 1965): if the  
274 function to minimize depends on  $N$  variables (the number of input parameters here), a simplex  
275 constituted by  $N + 1$  points is defined. The coordinates of the simplex are updated in turn so  
276 that the simplex vertices get closer to the local minimum. Even if this method gives little  
277 theoretical guarantees of convergence, it has proven to work well in practice (Lagarias et al.  
278 1998) and has the advantage that it does not require computing the gradient of each outflux  
279 with respect to each input parameter.

280 As the model takes 24 inputs and outputs 85 fluxes, concerns might be raised about the  
281 uniqueness of the solution found to minimize the term (1). To make the model identifiable, the  
282 number of input parameters to estimate is limited to the number of output fluxes available, here  
283 four. In this respect, the CFs have been fixed to  $0.5 \text{ kg C mol Leu}^{-1}$ . This value, contrary to the  
284 previously classically used value of  $1.55 \text{ kg C mol Leu}^{-1}$  (Simon and Azam 1989; Nagata et al.  
285 2010), was determined by Giering and Evans (2022) as the median value of 15 studies  
286 conducted in the mesopelagic zone. Doing so, we limit the number of free parameters to be  
287 estimated to four so that the model remains identifiable. The model is mostly linear and our  
288 experiments have shown the solution to be unique and independent of the initial values taken.

289 The codes and data to reproduce the results are available at  
290 <https://github.com/RobeeF/InverseCarbonBudgetEstim>

## 291 **3. Results**

### 292 **3.1 Most sensitive parameters**

293 Using Sobol indices, we identified the most sensitive parameters from the 24 of the Anderson  
294 and Tang (2010) model on the 4 fluxes outputs of the model for which we have the measured  
295 counterpart (i.e. PHP and PR of sinking prokaryotes, PHP of non-sinking prokaryotes and  
296 respiration of zooplankton). All parameter definitions are given in Table S1. For the outflux  
297 “PHP of non-sinking prokaryotes”, only the  $\text{PGE}_{\text{non-sinking}}$  appears to be sensitive with a Sobol  
298 index of 0.68 meaning that it explains 68% of the variance (Table 2). Fluxes related to sinking  
299 prokaryotes, i.e. their PHP and their PR, appear to be highly influenced both by  $\Psi$ ,  $\alpha$ , and



300  $PGE_{\text{sinking}}$  with indices of 0.22 and 0.23 for  $\Psi$ , 0.24 and 0.24 for  $\alpha$  and 0.27, 0.25 for  $PGE_{\text{sinking}}$   
 301 respectively. Surprisingly, zooplankton respiration is more impacted by the  $PGE_{\text{non-sinking}}$   
 302 (Sobol index of 0.52) than proper zooplankton parameters. All other parameters exhibit Sobol  
 303 indices below 1%. Total Sobol indices, indicating the part of the variance of fluxes due to the  
 304 parameter alone and in interaction with the others, were similar to the first-order indices,  
 305 suggesting no interactions of parameters regarding the variance of fluxes. This sensitivity  
 306 analysis enabled the identification of  $\Psi$ ,  $\alpha$ , and both PGEs as the most influential parameters,  
 307 suggesting that their values should be set with particular care. Especially for the  $PGE_{\text{non-sinking}}$   
 308 which can be responsible for more than 50% of the variance of  $PHP_{\text{non-sinking}}$  and zooplankton  
 309 respiration. PGEs are growth efficiencies defined as the amount of new prokaryotic biomass  
 310 produced per unit of organic C substrate assimilated and is a way to relate PHP and PR (del  
 311 Giorgio and Cole 1998).  $\Psi$  corresponds to the percentage of POC consumed by prokaryotes  
 312 and  $\alpha$  to the fraction of hydrolyzed POC which is lost into the surrounding water, i.e. not  
 313 assimilated by sinking prokaryotes that hydrolyzed it.

314 *Table 2: First-order Sobol indices for the parameters of the model by Anderson and Tang*  
 315 *(2010). The definition of each parameter can be found in Table S1. Significant Sobol indices*  
 316 *(>0.2) are shown in red. PHP and PR respectively refer to Prokaryotic Heterotrophic*  
 317 *Production and to Prokaryotic Respiration.*

	$\Psi$	$PGE_{\text{sinking}}$	$PGE_{\text{non-sinking}}$	$\alpha$	$\Phi_v$	$\beta_v$	$K_v$	$\Phi_z$	$\beta_z$	$K_z$	$\lambda_z$	$\Phi_h$	$\beta_h$	$\lambda_h$	$K_h$	$\zeta$	$\zeta_2$		
Non-sinking prokaryotes PHP	<0.01	0.021	0.681	0.01	<0.01	<0.01	<0.01	0.014	<0.01	0.011	-0.012	<0.01	0.015	<0.01	<0.01	<0.01	<0.01	<0.01	
Sinking prokaryotes PHP	0.222	0.24	<0.01	0.265	<0.01	<0.01	<0.01	<0.01	0.011	<0.01	<0.01	<0.01	<0.01	0.011	<0.01	<0.01	0.012	<0.01	-0.011
Sinking prokaryotes PR	0.225	0.243	<0.01	0.252	-0.019	<0.01	<0.01	<0.01	-0.011	<0.01	<0.01	<0.01	0.012	<0.01	<0.01	<0.01	<0.01	<0.01	<0.01
Zooplankton respiration	<0.01	0.023	0.507	<0.01	<0.01	0.014	<0.01	0.064	0.027	0.041	<0.01	<0.01	<0.01	<0.01	<0.01	0.028	<0.01	<0.01	<0.01

318

### 319 3.2 Model inversion



320  
321 The optimization method, described in the material and method section, enabled the  
322 determination of the 4 parameters identified as sensitive above:  $\Psi$ ,  $\alpha$ ,  $PGE_{\text{sinking}}$ , and  $PGE_{\text{non-}}$   
323  $\text{sinking}$  in the case study of PAP DY032. Table 3 reports the combination found by model  
324 inversion. By construction of the procedure (e.g. same number of input and output), the solution  
325 is unique, explaining why no confidence intervals are reported. The errors between the four  
326 fluxes generated by the model and their measured counterparts were less than 1%, far lower  
327 than potential measurement errors. The zooplankton flux was the best matched, followed by  
328 the PR of the sinking prokaryotes, the PHP of the non-sinking prokaryotes, and of the sinking  
329 prokaryotes.

330

331 *Table 3: Estimation of the parameters  $\Psi$ ,  $\alpha$ ,  $PGE_{\text{sinking}}$  and  $PGE_{\text{non-sinking}}$  obtained by inversion*  
332 *of the model by Anderson and Tang (2010). As the model was made identifiable, the solutions*  
333 *are unique, explaining the absence of confidence intervals. The remaining differences between*  
334 *the model outfluxes deriving from the estimated input values and the actual in situ*  
335 *measurements are referred to as “Errors” and are expressed in percentage. PHP, PR, and ZR*  
336 *respectively stand for Prokaryotic Heterotrophic Production, to Prokaryotic Respiration and*  
337 *to Zooplankton Respiration.*

Estimations				Errors			
$\Psi$	$\alpha$	$PGE_{\text{sinking}}$	$PGE_{\text{non-sinking}}$	$PHP_{\text{non-sinking}}$	$PHP_{\text{sinking}}$	$PR_{\text{sinking}}$	ZR
0.675	0.777	0.026	0.087	-0.487%	0.524%	0.184%	-0.05%

338

339

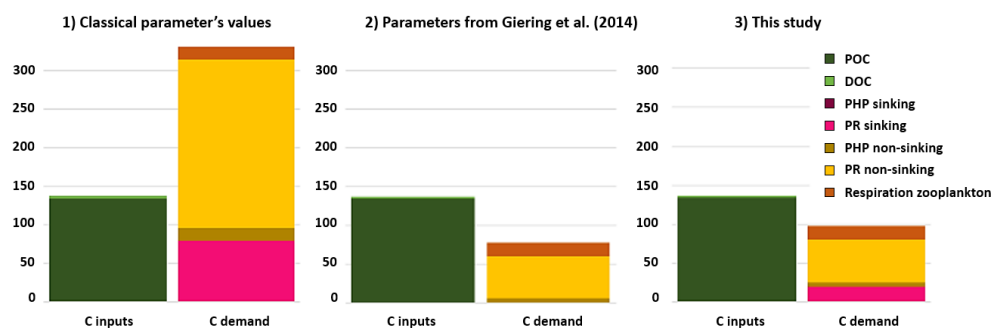
### 340 3.3 C budget

341

342 The two PGEs presented above along with CF of  $0.5 \text{ kg C mol Leu}^{-1}$  were applied to leucine-  
343 incorporation rates measurements to build the corresponding active mesopelagic C budget. The  
344 resulting C budget was compared with two other C budgets calculated with different sets of  
345 parameters. The three active mesopelagic zone C budgets resulting from DY032 measurements  
346 or estimation are represented in Fig. 1 with the budget (1) obtained with the classical CF value  
347 of  $1.55 \text{ kg C mol Leu}^{-1}$  and median literature values for PGEs, i.e. 0.07 for  $PGE_{\text{non-sinking}}$   
348 (Aristegui et al. 2005; Reinthaler et al. 2006; Baltar et al. 2010; Collins et al. 2015) and 0.02  
349 for  $PGE_{\text{sinking}}$  (Collins et al. 2015); the budget (2) obtained with the parameter values from  
350 Giering et al. (2014) who reconcile C budget, i.e. CF of  $0.44 \text{ kg C mol Leu}^{-1}$ ,  $PGE_{\text{non-sinking}}$  of



351 0.07, and  $PGE_{\text{sinking}}$  of 0.24 and the budget (3) obtained with a CF,  $PGE_{\text{sinking}}$  and  $PGE_{\text{non-sinking}}$   
352 of 0.5, 0.026 and 0.087, respectively, determined in this study. The combination yielding to the  
353 largest discrepancy is the budget (1) (Fig. 1) (discrepancy of  $-194 \text{ mg C m}^{-2} \text{ d}^{-1}$ ). The C input  
354 seems to support the zooplankton respiration and total C demand of sinking prokaryotes but  
355 not the one of non-sinking prokaryotes especially due to their PR of  $218 \text{ mg C m}^{-2} \text{ d}^{-1}$ .  
356 Combination of budget (2) and (3) presented both an excess of C (60 and  $40 \text{ mg C m}^{-2} \text{ d}^{-1}$   
357 respectively) compared to the biological C demand. These two differ mainly on the PR of  
358 sinking prokaryotes which is negligible in combination (2) but which is the second largest flux  
359 in the C demand in our study. In all cases, the C demand of non-sinking prokaryotes accounts  
360 for most of the total C demand.



361  
362 *Figure 1: Carbon budget for the active mesopelagic zone estimation resulting from DY032*  
363 *measurements or estimation and on which different combination of CF (1.55, 0.44 and 0.5 respectively*  
364 *for budget 1) 2) and 3)),  $PGE_{\text{sinking}}$  (0.02, 0.24 and 0.026 respectively for budget 1) 2) and 3)) and*  
365  *$PGE_{\text{non-sinking}}$  (0.07, 0.08 and 0.087 respectively for budget 1) 2) and 3)) were applied on leucine*  
366 *incorporation rates of sinking and non-sinking prokaryotes. See Fig. S1 for value details.*

## 367 4. Discussion:

368 As stated in the introduction, the scientific community has struggled to reconcile the  
369 mesopelagic carbon budget with measurements and estimates showing a carbon demand often  
370 greater than the amount of known organic C sources (e.g. Reinthaler et al. 2006; Steinberg et  
371 al. 2008; Burd et al. 2010; Collins et al. 2015; Boyd et al. 2019). Building C budget involves a  
372 plethora of parameters whose impacts are overlooked and often neglected, mainly because  
373 neither their ideal values nor their underlying mechanism in the water column across space and  
374 time are clearly understood. The scientific community is concerned about this issue (e.g. Burd  
375 et al. 2010; Giering and Evans 2022), but in the absence of a better option and in an attempt to  
376 encourage comparisons, the same parameter values are universally used. A first step towards



377 this direction was conducted thanks to the RUBALIZ method (Fuchs et al. 2022) which  
378 precisely determines the vertical location of the “active mesopelagic zone” and thereby  
379 estimates the boundaries between which to integrate C fluxes. In the current study, we pursue  
380 this investigation and combine measurements with modeling approaches to investigate the role  
381 of sensitive parameters related to the remineralization of POC in the mesopelagic zone.

#### 382 **4.1 Optimization method: Consistency of parameters estimated**

383 The Anderson and Tang (2010) model takes as inputs the measured C inputs as well as 24  
384 parameters related to the activity of organisms such as sinking prokaryotes, non-sinking  
385 prokaryotes, zooplankton detritivores, bacterivores, and carnivores. Among the 24 parameters,  
386 four have been found to be particularly sensitive in assessing the carbon demands of the various  
387 groups:  $\Psi$  (percentage of particle consumption by prokaryotes),  $\alpha$  (percentage of C hydrolyzed  
388 released in surrounding water),  $PGE_{\text{non-sinking}}$  and  $PGE_{\text{sinking}}$  (growth efficiencies of sinking and  
389 non-sinking prokaryotes). It is interesting to note that zooplankton respiration (which is the  
390 sum of detritivores, bacterivores and carnivores respiration) is mostly sensitive to one  
391 parameter:  $PGE_{\text{non-sinking}}$  but not to a parameter specific to zooplankton. This counter-intuitive  
392 result suggests a strong synergy between the two model compartments. At this point, it is  
393 challenging to establish whether this is the outcome of a complex ecological process or a model  
394 artifact.

395

396 In the model, the consumption of particles is done by two groups: prokaryotes ( $\Psi$ ) and  
397 detritivores ( $1-\Psi$ ). It can be estimated by taking the average ratio between PHP and ZR.  
398 Anderson and Ryabchenko (2009) estimated  $\Psi$  using calculations of POC consumption by  
399 prokaryotes and zooplanktons between 150 and 1000m performed by Steinberg et al. (2008) in  
400 the Pacific. Following this, they set  $\Psi$  at 0.76. The inversion of the Anderson and Tang model  
401 (2010) leads to a well-identified solution of  $\Psi$ , i.e. 0.67 in the case of PAP DY032 cruise. This  
402 value is in line with the one used by Anderson and Tang (2010). However, data are lacking to  
403 compare and explore variations of  $\Psi$  value across seasons, locations or depths. In the model,  $\Psi$   
404 participates in the repartition of POC input between prokaryotes and detritivores. Whether for  
405 modeling purposes to determine  $\Psi$  or to build a C-budget without a model, PHP and ZR are  
406 required. It remains too rare to have both together and more future efforts should be devoted to  
407 get PHP and ZR concomitantly.

408

409 Beyond  $\Psi$ , according to Sobol indices,  $\alpha$  is the second parameter of interest. Amino acids and  
410 sugar are major components of POC, constituting between 40 to 70% of POC in the



411 mesopelagic zone (Wakeham et al. 1997). When prokaryotes consume POC using hydrolytic  
412 enzymes, a major fraction of the hydrolyzed C is lost to the surrounding environment as DOC  
413 (Smith et al. 1992; Vetter et al. 1998). This loss is represented by  $\alpha$  and is very difficult to  
414 quantify accurately. Two major experiments, focused on amino acid hydrolysis, aimed to  
415 determine such losses: Smith et al. (1992) and Grossart and Ploug (2001). Smith et al. (1992)  
416 sampled particles at 25m and showed that 97% of particulate combined amino acids are  
417 released in the surrounding water. Later, Grossart and Ploug (2001) using aggregates from  
418 phytoplankton cultures show a loss of POC of 74%. Relying on these two studies, Anderson  
419 and Tang (2010) followed by Giering et al. (2014) consider that the value should be lower than  
420 that of a fresh detritus and choose a conservative value of 0.5. In the case of these two  
421 experiments, only the amino acids are considered and the experiments were conducted under  
422 laboratory-controlled settings. Conversely, we used unpublished data from PEACETIME  
423 cruise (see methods details in supp. data) of *in situ* hydrolysis rates of aminopeptidase and  $\beta$ -  
424 glucosydase from sinking prokaryotes (which hydrolyze amino acids and sugar, respectively)  
425 that we were able to convert into hydrolyzed carbon fluxes (see measurements and calculation  
426 details in supp. data). Unfortunately, total hydrolyzed C fluxes were most of the time below  
427 the C demand of the sinking prokaryotes which is unrealistic and probably due to the low  
428 amount of POC (sinking POC concentration of  $<1 \text{ mg L}^{-1}$  in the sinking fraction) resulting in  
429 insufficient sinking prokaryotes abundance to detect their activity by volume. However, when  
430 total hydrolyzed C fluxes were superior to  $\text{PHP}_{\text{sinking}}$  (indicating that some hydrolyzed C is not  
431 assimilated and is released),  $\alpha$  was estimated between 0.19 and 0.79 with a mean of  $0.41 \pm 0.24$   
432 and seems to decrease with depth (see calculations details in supp data). This could confirm  
433 Grossart and Ploug's (2001) work showing that the older a detritus is, the less enzymatic  
434 activity there is and therefore the less amino acid loss. Even if  $\alpha$  is not measurable easily, this  
435 parameter is identified at 0.78 by the inversion method during a post-bloom period at the PAP  
436 site. This value is consistent with Smith et al. (1992) and Grossart and Ploug (2001) evidencing  
437 high  $\alpha$  for surface aggregates (0.97) with laboratory-made phytoplankton aggregates (0.74), or  
438 with our calculations for the Mediterranean Sea ( $0.41 \pm 0.24$ ), an oligotrophic region. This  
439 suggests that the optimization method is a relevant alternative to determine  $\alpha$ . In addition,  $\alpha$   
440 corresponds to a release of C in the surrounding water. Regarding the model, the C demand of  
441 free-living prokaryotes matches the hydrolyzed C released which constitutes their main C  
442 sources. The relationship between enzymatic activities and heterotrophic production of free-  
443 living prokaryotes is well documented in the deep-sea ocean (Cho and Azam 1988; Smith et  
444 al. 1992; Hoppe and Ullrich 1999; Tamburini et al. 2002, 2003; Nagata et al. 2010). Total C  
445 demand of non-sinking prokaryotes is challenging to measure due to the diversity of existing



446 methods, especially the PR (e.g. Table S2), which leads to an incredibly wide range of  
447 estimated values. Subsequently, identifying  $\alpha$  via the optimization method could help to avoid  
448 these conflicting PR measurements.

449

450 The last two sensitive parameters according to Sobol indices were  $PGE_{\text{non-sinking}}$  and  $PGE_{\text{sinking}}$ .  
451 A wide range of  $PGE_{\text{non-sinking}}$  has been estimated using  $PHP_{\text{non-sinking}}$  and  $PR_{\text{non-sinking}}$  in the open  
452 ocean (e.g. Sherry et al. 1999; Lemée et al. 2002; Carlson et al. 2004; Arístegui et al. 2005;  
453 Reinthaler et al. 2006; Baltar et al. 2009, 2010; Collins et al. 2015). Overall it varies from 0.001  
454 to 0.64 (Collins et al. (2015) and Sherry et al. (1999), respectively). However, these values  
455 were produced from different protocols for the PHP (changes in biomass, thymidine or leucine  
456 incorporation, each with its own conversion factors and/or constants) and for the PR methods  
457 (by ETS measurements, micro-winkler titration, changes in dissolved  $O_2$ , or using optodes  
458 sensors spots, see Table S2) and correspond to various locations, seasons and depths. These are  
459 all valid reasons that can potentially explain the stark contrast in the values reported. If one  
460 focuses only on the mesopelagic zone in the North Atlantic, the median is 0.07 (Arístegui et al.  
461 2005; Reinthaler et al. 2006; Baltar et al. 2010; Collins et al. 2015). The optimization method  
462 yielded to a value of 0.087 and therefore produces very consistent results for a post-bloom  
463 period at the PAP site. Concerning  $PGE_{\text{sinking}}$ , too few values are available. To our knowledge,  
464 only Collins et al. (2015) provided *in situ* values associated with sinking prokaryotes (from  
465 0.01 to 0.03) at 150m. This is the only comparison we have, and our value of 0.026 matches  
466 this order of magnitude. To provide further comparison, the DY032 data before integration  
467 allows us to calculate a  $PGE_{\text{sinking}}$  (using  $PGE_{\text{sinking}} = \frac{PHP_{\text{sinking}}}{(PHP_{\text{sinking}} + PR_{\text{sinking}})}$  from del  
468 Giorgio and Cole 1998) per  $PR_{\text{sinking}}$  and  $PHP_{\text{sinking}}$  of sinking prokaryotes points performed at  
469 the same depth. This led to a variation from 0.033 at 70m to 0.0013 at 500m. Although the lack  
470 of datapoints deeper than 500m and the low number of points forces us to stay cautious about  
471 these estimates, it may indicate that  $PGE_{\text{sinking}}$  is not constant throughout the mesopelagic zone  
472 and decreases with depth. Constraining conditions due to the increase of hydrostatic pressure  
473 and decrease in temperature experienced by prokaryotes attached to sinking particles could  
474 explain this decrease in  $PGE_{\text{sinking}}$  (Stief et al. 2021; Tamburini et al. 2021). Under highly  
475 constrained conditions, Russell and Cook (1995) explained that maintaining respiration at the  
476 highest possible rate would allow the supply of active membrane transporters which are vital  
477 to the cell. This implies a low but optimal PGE (Westerhoff et al. 1983) which could thus  
478 decrease with depth and time as the POC becomes less labile (Grossart and Ploug 2000). On  
479 the contrary, the Anderson and Tang (2010) model, and the associated model inversion  
480 presented here, is built so that the mesopelagic zone is considered as one homogeneous entity.





481 Explicitly, specifying depth-dependent  $PGE_{\text{sinking}}$  in the mesopelagic zone could lead to more  
482 realistic modeling, but would entail a non-negligible additional model complexity.

483

484 It is worth noting that the  $PGE_{\text{sinking}}$  and  $PGE_{\text{non-sinking}}$  estimated here rely on a leucine-to-carbon  
485 Conversion Factor (CF) of  $0.5 \text{ kg C mol Leu}^{-1}$ . This value comes from the median of 15 values  
486 obtained on the free-living prokaryotes of the mesopelagic zone (between 300 to 1000m),  
487 which do not sink and are adapted to their place in the water column (Giering and Evans 2022).  
488 However, to our knowledge, there are no such values measured for the specific case of sinking  
489 prokaryotes. The latter are surface prokaryotes that have attached to the particles and will  
490 experience changes in conditions (e.g. pressure, temperature) linked to their sink (Baumas et  
491 al. 2021; Tamburini et al. 2021). The CF depends, among other things, on the leucine fraction  
492 in the proteins and the cellular carbon/protein ratio (Kirchman and Ducklow 1993). It is known  
493 that stresses can affect the incorporation of leucine into proteins and general protein production  
494 (e.g. Young 1968; Welch et al. 1993) and that these parameters can vary with prokaryotic  
495 diversity, especially between bacteria and archaea (Bogatyreva et al. 2006). Stresses occur  
496 during the descent throughout the water column and sinking prokaryotes experienced a drastic  
497 decrease in diversity following the sink at PAP DY032 (Baumas et al. 2021; Tamburini et al.  
498 2021). We can therefore easily imagine that the CF for sinking prokaryotes could be impacted.  
499 Despite this, without having further data, we applied the same CF on sinking as the 0.5  
500 recommended by Giering and Evans (2022) for non-sinking prokaryotes and the results were  
501 consistent.

502

## 503 **4.2 Influence on mesopelagic C Budget**

504 As stated in the introduction, mesopelagic C budgets are constructed by applying a CF and a  
505 PGE on leucine incorporation rates data to assess prokaryotic C demand. In Fig. 1, we applied  
506 three different combinations of CFs and PGEs to the same data. The combination using  
507 conventional CF of  $1.55 \text{ kg C mol Leu}^{-1}$ ,  $PGE_{\text{non-sinking}}$  of 0.07, and  $PGE_{\text{sinking}}$  of 0.02 led to an aberrant  
508 discrepancy such that more than the entire C pool would be remineralized in the active  
509 mesopelagic zone and that there would be no source of C to sustain deeper zone life nor  
510 sequestration by the BCP. As stated above, this was a recurrent issue in the field (Reinthal et  
511 al. 2006; Steinberg et al. 2008; Burd et al. 2010; Collins et al. 2015; Boyd et al. 2019) with the  
512 exception of Giering et al. (2014) who reconcile the C budget of the mesopelagic zone.  
513 Although Giering et al. (2014) did not take into account sinking prokaryotes from *in situ* data  
514 point of view, their results were mainly due to the difference in CF used, i.e.  $0.44 \text{ kg C mol Leu}^{-1}$



515 <sup>1</sup>. However, from a model point of view, the main difference between C budgets estimated  
516 using Giering et al. (2014) parameters and those determined by our optimization method is due  
517 to the 10-fold difference between  $PGE_{\text{sinking}}$  used. Giering et al. (2014) used 0.24 which is the  
518 mean of a 14 days incubation experiment during which PGE varied from 0.45 in the first 3 days  
519 to 0.04 at the end for riverine aggregates (Grossart and Ploug 2000). Despite the fact that  
520  $PGE_{\text{sinking}}$  data are very scarce, riverine values of 0.24 seem highly unlikely and inappropriate  
521 to mesopelagic sinking prokaryotes compared to what is known in marine environments (e.g.  
522 Collins et al. 2015). Indeed, if we consider that enzymes account for a large proportion of the  
523 proteins produced by cells (see above) the  $PGE_{\text{sinking}}$  must be low due to the high metabolic  
524 cost of their production (Grossart and Ploug 2000). Finally, the C budget built from a  
525 combination of CFs of  $0.5 \text{ kg C mol Leu}^{-1}$  and PGEs revealed by our optimization method seems  
526 the most reasonable option (from the three budgets built, Fig. 1) with an excess of C input of  
527  $40 \text{ mg C m}^{-2} \text{ d}^{-1}$ . In this case, PGEs were determined by the model, which in addition to PHP  
528 and PR of sinking and non-sinking prokaryotes and zooplankton respiration, also accounts for  
529 the production of zooplankton biomass into calculations. We do not have measurements or  
530 estimates for the production of zooplankton biomass but based on the model, this biomass  
531 production is  $11 \text{ mg C m}^{-2} \text{ d}^{-1}$ . Adding this value to the C demand implies a leftover of  $29 \text{ mg}$   
532  $\text{C m}^{-2} \text{ d}^{-1}$  that is not used and is exported under the active mesopelagic zone via gravitational  
533 sinking POC. This value is in accordance with the POC flux estimated from measures at 751m  
534 (thus at the exit of our zone):  $17 \text{ mg C m}^{-2} \text{ d}^{-1}$ . Being aware of the biases that may exist in the  
535 fluxes used as well as in the construction of the model itself, our optimization method enables  
536 the determination of realistic values of parameters and thus constructing robust C budgets. As  
537 far as we know, the combination of field measurements (using consistently defined integration  
538 depths, such as RUBALIZ (Fuchs et al. 2022) with the use of optimization method on the  
539 Anderson & Tang model has led to the most complete and realistic mesopelagic carbon budget.  
540

### 541 **4.3 Model: reliability and potential biases**

542 The Anderson and Tang model (Anderson and Tang 2010) was originally parametrized with  
543 24 input parameters and 85 output fluxes, and is hence by definition an underdetermined model  
544 as the number of outputs is higher than the number of inputs. To make the model identifiable,  
545 i.e. obtaining unique solutions for each parameter value, the number of parameters allowed to  
546 vary, namely:  $\Psi$ ,  $\alpha$ ,  $PGE_{\text{non-sinking}}$ , and  $PGE_{\text{sinking}}$ , was restricted to the number of measurable  
547 outputs (here four,  $PHP_{\text{sinking}}$ ,  $PR_{\text{sinking}}$ ,  $PHP_{\text{non-sinking}}$ , and zooplankton respiration).  
548 Measurement errors (e.g. measurement device errors, *in situ* variabilities, errors due to



549 integration methods) are typically challenging to characterize. Furthermore, even if these four  
550 outfluxes well describe the prokaryotic and zooplankton compartment fluxes, one may wonder  
551 about the sensitivity of the results to the fact that a given outflux is not available or estimated  
552 with error.

553

554 As a result, we have tested two settings: a model inversion without the zooplankton respiration  
555 flux (using only three fluxes) and a second setting where the PGEs were estimated from the  
556 leucine incorporation rate using freely varying CFs, i.e. with CFs no more fixed at 0.5 as a  
557 value. The results are reported in Table S3 and S4. Not using the zooplankton flux to inverse  
558 the model mechanically adds some variability to the estimation results, especially concerning  
559  $\Psi$ ,  $\alpha$ , and  $\text{PGE}_{\text{non-sinking}}$ , in decreasing order of variability (Table S3). The  $\text{PGE}_{\text{sinking}}$  was not  
560 affected as its confidence interval length was inferior to  $10^{-7}$ : this underlines the very limited  
561 influence between the zooplankton and sinking prokaryote compartments in the model  
562 (contrary to the zooplankton and non-sinking prokaryote compartments). Yet, the difference  
563 between the four-flux and three-flux parameter estimations was negligible (<1% variation for  
564 each estimate), highlighting the robustness of the estimates to the potential unavailability of  
565 the zooplankton respiration. On the contrary, as made visible in Table S4, not fixing the CFs  
566 to estimate the PGEs created more variations in the PGE estimations, while the estimations of  
567  $\Psi$  and  $\alpha$  changed by less than 5% with respect to Table 2 estimations. The PGEs of the attached  
568 and free-living parameters get significantly closer to their fixed boundaries (10%), while the  
569 CFs rise, especially the CF of the attached particles (=1.865). Similarly, if PGEs are no longer  
570 bounded, the estimates of PGEs (0.173 for attached prokaryotes and 0.226 for free-living  
571 prokaryotes) and CFs (3.927 for attached prokaryotes and 1.526 for free-living prokaryotes)  
572 become unrealistic. This can be explained by the fact that the PGEs and CFs play similar roles  
573 in the current formulation of the model. Hence, without additional fluxes ensuring full model  
574 identifiability, one of these two types of quantities needs to be fixed to estimate the other.

575

576 In addition to these sensitivity analyses, an uncertainty analysis has been run by simulating  
577 errors in the measurements of the POC, DOC and the four output fluxes (see Table S5 in supp.  
578 data). Simulating errors from -10% to 10% for each flux, the estimation of the four parameters  
579 of interest were lowly affected: 1%, 2%, 3% and 1% on average for the  $\Psi$ ,  $\text{PGE}_{\text{sinking}}$ ,  $\text{PGE}_{\text{non-}}$   
580  $\text{sinking}$  and  $\alpha$ , respectively. The  $\text{PGE}_{\text{non-sinking}}$  was mostly sensitive to measurement errors of POC  
581 flux, DOC flux and  $\text{PHP}_{\text{non-sinking}}$  (generating variations of 6%, 5% and 5%, respectively).  
582 Similarly, the  $\text{PGE}_{\text{sinking}}$  was logically mostly sensitive to errors in the  $\text{PHP}_{\text{sinking}}$  and  $\text{PR}_{\text{sinking}}$



583 (generating variations of 6% for both). For the measurement errors, the generated variations all  
584 remained under 3% which is reassuring concerning the stability of the estimation.

585

586 Finally, the last potential source of estimation bias results from the assumed stationarity  
587 hypothesis of the mesopelagic system. For logistical and technical reasons, measurements and  
588 sampling between the upper and lower boundary of the mesopelagic zone are typically  
589 performed simultaneously. The stationarity assumption is thus a natural foundation ground  
590 upon interpretations and models. However, there is a temporal delay in flux variations between  
591 the upper layer and lower measurements (Giering et al. 2017; Stange et al. 2017). This delay  
592 depends on the particles sinking speed typically ranging from 2 to 1500 m d<sup>-1</sup> (Alldredge and  
593 Silver 1988; Armstrong et al. 2002; Trull et al. 2008; Turner 2015), their morphotype, density  
594 and porosity as well as the timing of their production. Strong meteorological events can also  
595 perturbate C fluxes from the water column with an increasing time lag over depth (e.g. Pedrosa-  
596 Pàmies et al. 2019). Admittedly, C budgets suffer from lack of time integration into the  
597 analysis. Our study regarding PAP site is also concerned as it undergoes a substantial  
598 seasonality (Cole et al. 2012; Giering et al. 2017). Although, we do not have enough  
599 understanding of vertical time lag to change the model and to avoid such bias yet. Some long-  
600 term observatories such as BATS in the Bermuda Atlantic or HOT in Hawaii provide  
601 biogeochemical flux time series but monthly sampling focuses mostly on the euphotic zone  
602 and does not investigate the mesopelagic zone enough. Sampling at discrete times following  
603 the sink of a bloom (e.g. Le Moigne et al. 2016) could be a solution, which would nevertheless  
604 entail a significant cruise planning effort.

605

## 606 **4.4 Grounds for improvements**

607 Anderson & Tang model allowed us to have a comprehensive vision of the remineralization  
608 processes in the mesopelagic zone by including the interactions between various  
609 compartments, completing *in situ* measurements with a comprehensive vision of the  
610 mechanisms at stake. The described inversion of the Anderson & Tang model provided  
611 meaningful estimations of the parameters of interest. However, as most models represent  
612 complex phenomena, some processes are not fully and properly captured by the model. Below,  
613 we provide a list of processes that may help refining mesopelagic C budget estimations.

614

### 615 **4.4.1 Other microorganisms**



616 Are not included in the model, the role of microbial eukaryotes, viruses, and the input of C by  
617 chemolithotrophs whose potential role has gained in importance (Herndl and Reinthaler 2013;  
618 Lara et al. 2017; Kuhlisch et al. 2021; Luo et al. 2022). For instance, eukaryotes can dominate  
619 microbial biomass on bathypelagic particles (Bochdansky et al. 2017), and have the potential  
620 to promote the aggregation of particles (Jain et al. 2005; Chang et al. 2014; Hamamoto and  
621 Honda 2019; Xie et al. 2022). Viruses could be the main cause of prokaryotic and  
622 phytoplanktonic mortality. Thus, DOC fluxes could be attributed to them, in particular with the  
623 cell lyses they provoke (Fuhrman 2000 and ref within, Lara et al. 2017; Kuhlisch et al. 2021).  
624 In the North Atlantic, 9 to 12% of cells could be infected by viruses which would cause a DOC  
625 production of  $0.1 \text{ mg C m}^{-3} \text{ d}^{-1}$  (Wilhem and Suttle 1999). For comparison, PHP results on PAP  
626 before integration (with a conversion factor of  $0.5 \text{ kg C mol}^{-1} \text{ Leu}$ ) were mostly below this  
627 value. In addition, inorganic C fixation by chemoautotrophy would be of the same order of  
628 magnitude as  $\text{PHP}_{\text{non-sinking}}$  rates (Herndl et al. 2005; Reinthaler et al. 2010). It would be  
629 important to verify what microbial eukaryotes, chemolithotrophs or viruses contributions are,  
630 even if the poor understanding of these processes currently prevents properly integrating them  
631 into models.

632

#### 633 **4.4.2 Lifestyles**

634 More surprisingly, sinking prokaryotes are poorly considered as they are not sampled with the  
635 Niskin bottles classically used in oceanography (Planquette and Sherrell 2012; Baumas et al.  
636 2021). However, the use of the MSC at PAPDY032 allows us to access fractions of particulate  
637 organic carbon that will allow us to evaluate the importance of sinking prokaryotes. We have  
638 seen that their C demand is not negligible and represents 18% of total C demand. Anderson &  
639 Tang model distinguishes sinking particles from neutrally buoyant particles, each with distinct  
640 attached communities. Since sampling with MSC only allows us to separate what is sinking  
641 from what is not, we merged free-living prokaryotes with those attached to neutrally buoyant  
642 particles without distinction. However, unlike free-living prokaryotes, prokaryotes attached to  
643 neutrally buoyant particles have access to POC and must produce enzyme activity with  
644 different metabolisms than their free-living counterparts. On the other hand, prokaryotes  
645 attached to neutrally buoyant particles are also different from prokaryotes attached to sinking  
646 particles since they do not undergo changes in temperature and pressure related to the sink.  
647 They must therefore surely have intrinsically different PGE and associated remineralization  
648 rates. It would therefore be valuable to consider them as a third distinct group in laboratory  
649 experiments and sampling. Contrary to the sinking or ascending particles which are naturally  
650 split by their sinking/ascending velocity (e.g. respectively Smith et al. 1989; Cowen et al. 2001;



651 McDonnell et al. 2015), no means allow the selective and exclusive sampling of neutrally  
652 buoyant particles. The only valid way is to use the MSC to let the sinking particles fall into the  
653 lower compartments and to filter the "non-sinking" part to retain the particulate fraction.  
654 However, it is known that filtration affects the activities of prokaryotes and generates biases  
655 (Edgcomb et al. 2016). This makes investigations of prokaryotes associated with neutrally  
656 buoyant particles particularly challenging and future endeavors should urgently attempt to  
657 target them.

658

#### 659 **4.4.3 OC inputs**

660 Continuing in the same line, the inputs of C that the model takes into account are only the  
661 gravitational POC and the DOC. We chose to artificially increase the gravitational POC flux  
662 to add sources of neutrally buoyant particles in the form of PIPs (eddy subduction pump,  
663 metazoans migrations and large-scale physical pumps). Indeed, Boyd et al. (2019) clearly  
664 showed that these PIPs can be of paramount importance (here we have estimated them at 51.6%  
665 of the gravitational flux). Accounting for these neutrally buoyant particles through the POC  
666 flux was performed due to the model structure. Yet, explicitly describing them in a dedicated  
667 compartment of the model could be an improvement for future research, as these neutrally  
668 buoyant particles have an effect on the whole system, including the prokaryotes linked to  
669 various types of particles and their predators or on particle fragmentation. Given the existence  
670 of the neutrally buoyant particle compartment, it is feasible to adapt the model to account for  
671 these C inputs. This is even more relevant as new optical instruments have flourished (e.g.  
672 Briggs et al. 2013; Giering et al. 2020; Picheral et al. 2022) and would make it easier to better  
673 quantify these neutrally buoyant particle fluxes.

674

#### 675 **4.4.4 *In situ* pressure effect**

676 Our last major concern deals with the fact that neither Niskin nor MSC avoid disruption  
677 introduced through the process of depressurization when samples are collected at depth  
678 (Tamburini et al. 2013; Garel et al. 2019). Heterotrophic activities associated to non-sinking  
679 prokaryotes are known to decrease with depth but were mostly sampled without taking care of  
680 the *in situ* pressure (e.g. Turley and Mackie 1994; Arístegui et al. 2009). From our knowledge,  
681 some devices such as the IODA<sub>6000</sub> (Robert 2012) were specifically designed to measure *in situ*  
682 PR of non-sinking prokaryotes. However, enigmatically high PR values (2-3 orders of  
683 magnitude higher than PHP) are measured by IODA<sub>6000</sub>, making it difficult to have confidence  
684 in these *in situ* measured PR rates. During the PEACETIME cruise, we use a pressure-retaining



685 sampler (methods presented in supp data), allowing for the first time to access both  $PHP_{non-}$   
686  $sinking$  and  $PR_{non-sinking}$  rates and to compare it with classical depressurization procedures (Fig.  
687 S1). We observed that activity rates of non-sinking prokaryotes kept under pressure were  
688 always higher when kept at *in situ* hydrostatic pressure than their decompressed counterparts  
689 and, surprisingly, seem to increase with depth rather than decrease typically depicted and found  
690 when the samples are decompressed (Fig. S1). Focusing on  $PR_{non-sinking}$  rates, obtained values  
691 are also several orders of magnitude too high to be realistic in regard to C-Budgets and prevent  
692 us from calculating PGEs. As PHP and PR are linked, it is very likely that the pressure effect  
693 (here, an increase) is reflected on both and thus in the associated  $PGE_{non-sinking}$ . Taking  
694 hydrostatic pressure into account could thus drastically affect C-budgets and even for  
695 zooplankton respiration as we saw in the model that they are really sensitive to  $PGE_{non-sinking}$ .  
696 We highly recommend using either direct *in situ* measurements or pressure retaining systems  
697 for future research. This advice should be followed carefully, especially from 500m where the  
698 pressure effect starts to be very important (Fig. S1), while the piezosphere was previously  
699 considered below 1000m depth (Jannasch and Taylor 1984; Yayanos 1986). Furthermore, this  
700 shows the crucial interest to measure points below 500m in order to get a global trend of the  
701 profile, which could not have been done here for sinking prokaryotes (the MSC were deployed  
702 only up to 500m during the cruise DY032). From a C-budget point of view, taking *in situ*  
703 pressure into account will increase C demand of free-living prokaryotes well adapted to their  
704 living depth.

705

706 The effect of pressure acts inversely on sinking prokaryotes, as they are surface prokaryotes  
707 (unadapted to high-hydrostatic pressure) that undergo a dynamic pressure increase as the  
708 particle sinks (Baumas et al. 2021; Tamburini et al. 2021). Besides, repeated results (Tamburini  
709 et al. 2006, 2009, 2021; Riou et al. 2018) have shown that, while performing a sinking  
710 simulation experiment the activities of sinking prokaryotes are affected during the sink. For  
711 instance, they noticed that the aminopeptidase activity was always lower with increasing  
712 pressure over time than at atmospheric pressure on diatom aggregates (Tamburini et al. 2006).  
713 This may reflect the stress endured by the sinking prokaryotes as they experience the sink. This  
714 could also be another explanation of why the fraction of hydrolyzed C released ( $\alpha$ ) tends to  
715 decrease with depth as it is directly linked with aminopeptidase activity. In view of these  
716 statements, it is not surprising that the PHP and PR, and therefore a PGE, are impacted by  
717 increasing pressure (e.g. Stief et al. 2021; Tamburini et al. 2021). Only the RESPIRE from  
718 Boyd et al. (2015) provides *in situ* measurements of the PR of sinking prokaryotes. However,  
719 in line with the previous comments, it gives unrealistically rather high values. Thus, sinking



720 simulation experiments remains, in the present, the best alternative to understand the mechanics  
721 of sinking prokaryotes during the sink of their associated particle. Several systems exist to  
722 simulate the sink (e.g. de Jesus Mendes et al. 2007; Grossart and Gust 2009; Tamburini et al.  
723 2009; Mendes and Thomsen 2012; Dong et al. 2018; Stief et al. 2021; Liu et al. 2022), all  
724 showing a general tendency that hydrostatic pressure affects activities (and diversity) of  
725 surface-originated prokaryotes, decreasing the integrated C-demand when taking into account.  
726 Handling high-pressure sampling or experiments requires much more effort and material than  
727 usual methods. However, it seems highly worthy when investigating both, sinking and non-  
728 sinking prokaryotes activities, in regard to C-budget purposes.

729

## 730 5. Conclusion

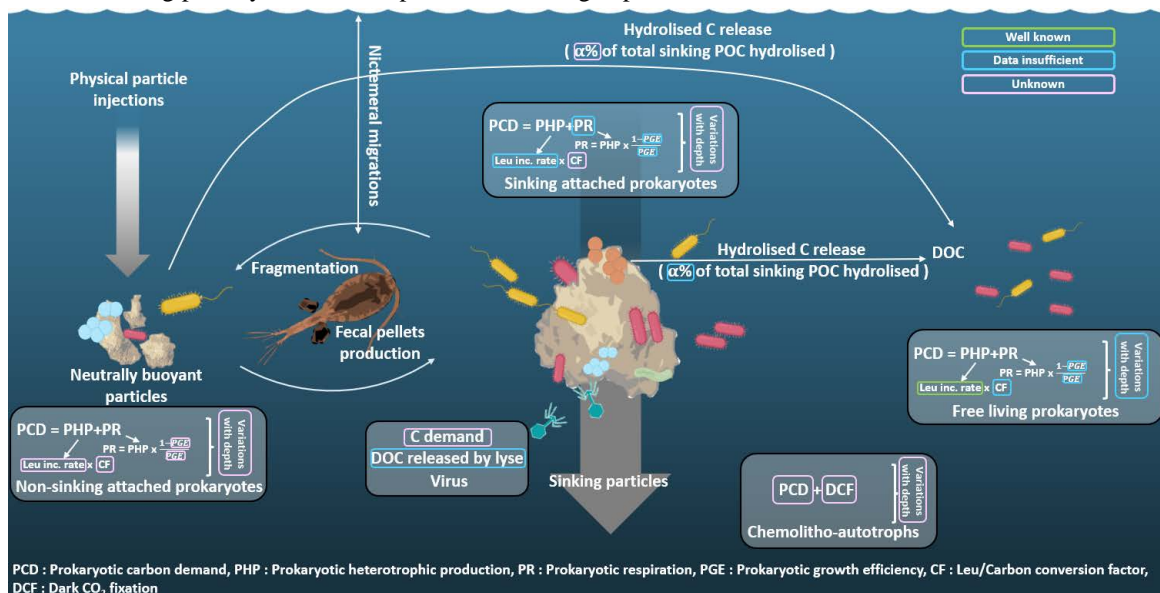
731 By combining *in situ* data from the DY032 cruise at the PAP site with inversion of the  
732 Anderson & Tang model which includes known processes from the biological C pump, we  
733 provide robust and ecologically realistic estimates of key parameters and to better characterize  
734 the patterns at stake.

- 735 1) We showed that the most sensitive parameters in the model are the ones related to  
736 prokaryotes such as prokaryotic growth efficiencies, leucine-to-carbon conversion  
737 factor, and C hydrolyzed by sinking prokaryotes released to the surrounding water.
- 738 2) By inversion of Anderson and Tang's model, we determined consistent values of the  
739 parameters listed above.
- 740 3) We showed that using these values instead of the classical mean from literature or  
741 inadequate theoretical values resulted in a more consistent and realistic C-budget than  
742 previously considered.
- 743 4) Additional measurements are needed to better understand both prokaryotic growth  
744 efficiencies and Leucine-to-Carbon conversion factors in the mesopelagic zone.  
745 However, we recommend measuring fewer fluxes for which we are confident  
746 associated with inversion model procedures in order to access parameter values  
747 challenging to measure in other places, cruises, or seasons.





748 Fig. 2 summarizes processes involved in mesopelagic C budgets estimations and highlights  
 749 missing knowledges. We attempt to classify the processes according to their degree of  
 750 understanding (well known, insufficient data or unknown) and point out that majority of these  
 751 processes require a better understanding. Among others, it is crucial to quantify the roles of  
 752 microbial eukaryotes, viruses, and chemoautotrophs in the entire process of C budgets.  
 753 Suspended particles should have a dedicated well-identified compartment in future studies  
 754 instead of being neglected and drowned into others. Finally, accounting for *in situ* hydrostatic  
 755 pressure when studying prokaryotic C demand is key. This is because: 1) it may reduce PCD  
 756 for sinking prokaryotes unadapted to increasing pressure and 2) it may increase PCD for free-  
 757 living prokaryotes well-adapted to their living depth.



758 Figure 2: Sinking particles export carbon (C) down to the mesopelagic zone through gravitational POC  
 759 fluxes where this latter is attenuated to satisfy C demand of different groups of organisms such as  
 760 prokaryotes living attached to sinking particles, attached to non-sinking particles, or free-living  
 761 prokaryotes. In turn, viruses and chemoautotrophs can increase the amount of usable labile C.  
 762 Quantifying C demand and role on POC fluxes of these different groups is crucial to truly assess C  
 763 sequestration in the deeper layer of the water column. However, a multitude of uncertainties remains  
 764 for each group. The quantities enclosed in green are well known, in blue lack data and in pink are  
 765 unknown. C demand is the sum of heterotrophic production (PHP) and respiration (PR). The  
 766 understanding of these two quantities is currently better for the free-living prokaryotes whereas data  
 767 are still insufficient for sinking prokaryotes and even absent for prokaryotes attached to non-sinking  
 768 particles. Moreover, to build C budgets, these variables are integrated over a few hundred meters of  
 769 water column and the relationship between *in situ* pressure and C demand remains often neglected even  
 770 if this relationship highly depends on the prokaryote type considered (not constant for sinking



771 *prokaryotes unadapted to the increased pressure, constant for free-living prokaryotes well adapted to*  
772 *their living depth and constant for prokaryotes attached to non-sinking particles which can be adapted*  
773 *or not if the particle was sinking before being stopped in its sink ).*  
774

## 775 **Code/Data availability**

776 The codes and data to reproduce the results are available at  
777 <https://github.com/RobeeF/InverseCarbonBudgetEstim>

## 778 **Author contribution**

779 The idea was conceived by CB, CT and JCP. Sampling and experiments onboard PEACETIME  
780 cruise were conducted by CT and MG. The data processing of PAP DY032 data was conducted  
781 by CB with advices from FLM, and the one from PEACETIME data by CB and MG. RF  
782 designed the inversion detection methodology and performed the estimation with advices from  
783 LM. CB and RF led the writing with significant contributions from all authors.

784

## 785 **Acknowledgement**

786 We thank the crew and officers of the R.R.S. DISCOVERY (NERC) for their help during the  
787 PAP DY032 cruise and of the N/O Pourquoi Pas? during the PEACETIME cruise. This study  
788 is a contribution to the PEACETIME project (MISTRALS CNRS INSU, doi:  
789 10.17600/17000300) managed by Cécile Guieu (LOV) and Karine Desboeufs (LISA). We  
790 warmly thank F. Van Wambeke, S. Guasco and B. Zancker for onboard works (enzymatic  
791 activities, sugar and amino acids concentrations measurements) during PEACETIME cruise.  
792 We wish to express our gratitude to F. Van Wambeke, S. Giering, T. Anderson and A. Belcher  
793 for stimulating and informative discussions. This manuscript is a contribution of the APERO  
794 project funded by the National Research Agency under the grant APERO [grant number ANR  
795 ANR-21-CE01-0027] and by the French LEFE-Cyber program.

## 796 **Competing interests**

797 The authors declare that they have no conflict of interest.



## 798 **References**

- 799 Alldredge, A. L., and M. W. Silver. 1988. Characteristics, dynamics and significance of  
800 marine snow. *Progress in Oceanography* **20**: 41–82. doi:10.1016/0079-  
801 6611(88)90053-5
- 802 Anderson, T. R., and V. A. Ryabchenko. 2009. Carbon cycling in the Mesopelagic Zone of  
803 the central Arabian Sea: Results from a simple model. Washington DC American  
804 Geophysical Union Geophysical Monograph Series **185**: 281–297.  
805 doi:10.1029/2007GM000686
- 806 Anderson, T. R., and K. W. Tang. 2010. Carbon cycling and POC turnover in the  
807 mesopelagic zone of the ocean: Insights from a simple model. *Deep Sea Research*  
808 Part II: Topical Studies in Oceanography **57**: 1581–1592.  
809 doi:10.1016/j.dsr2.2010.02.024
- 810 Arístegui, J., C. M. Duarte, J. M. Gasol, and L. Alonso-Sáez. 2005. Active mesopelagic  
811 prokaryotes support high respiration in the subtropical northeast Atlantic Ocean.  
812 *Geophysical Research Letters* **32**: 1–4. doi:10.1029/2004GL021863
- 813 Arístegui, J., J. M. Gasol, C. M. Duarte, and G. J. Herndl. 2009. Microbial oceanography of  
814 the dark ocean's pelagic realm. *Limnology and Oceanography* **54**: 1501–1529.  
815 doi:10.4319/lo.2009.54.5.1501
- 816 Armstrong, R. A., C. Lee, J. I. Hedges, S. Honjo, and S. G. Wakeham. 2002. A new,  
817 mechanistic model for organic carbon fluxes in the ocean based on the quantitative  
818 association of POC with ballast minerals. *Deep Sea Research Part II: Topical Studies*  
819 *in Oceanography* **49**: 219–236. doi:10.1016/S0967-0645(01)00101-1
- 820 Baltar, F., J. Arístegui, J. M. Gasol, E. Sintes, and G. J. Herndl. 2009. Evidence of  
821 prokaryotic metabolism on suspended particulate organic matter in the dark waters of  
822 the subtropical North Atlantic. *Limnology and Oceanography* **54**: 182–193.  
823 doi:10.4319/lo.2009.54.1.0182
- 824 Baltar, F., J. Arístegui, E. Sintes, J. M. Gasol, T. Reinthaler, and G. J. Herndl. 2010.  
825 Significance of non-sinking particulate organic carbon and dark CO<sub>2</sub> fixation to



- 826 heterotrophic carbon demand in the mesopelagic northeast Atlantic. *Geophysical*  
827 *Research Letters* **37**: n/a-n/a. doi:10.1029/2010GL043105
- 828 Baumas, C. M. J., F. A. C. Le Moigne, M. Garel, and others. 2021. Mesopelagic microbial  
829 carbon production correlates with diversity across different marine particle fractions.  
830 *The ISME Journal* **15**: 1695–1708. doi:10.1038/s41396-020-00880-z
- 831 Belcher, A., M. Iversen, S. Giering, V. Riou, S. A. Henson, L. Berline, L. Guilloux, and R.  
832 Sanders. 2016. Depth-resolved particle-associated microbial respiration in the  
833 northeast Atlantic. *Biogeosciences* **13**: 4927–4943. doi:10.5194/bg-13-4927-2016
- 834 Bochdansky, A. B., M. A. Clouse, and G. J. Herndl. 2017. Eukaryotic microbes, principally  
835 fungi and labyrinthulomycetes, dominate biomass on bathypelagic marine snow. *The*  
836 *ISME Journal* **11**: 362–373. doi:10.1038/ismej.2016.113
- 837 Bogatyreva, N. S., A. V. Finkelstein, and O. V. Galzitskaya. 2006. Trend of amino acid  
838 composition of proteins of different taxa. *J. Bioinform. Comput. Biol.* **04**: 597–608.  
839 doi:10.1142/S0219720006002016
- 840 Boyd, P. W., H. Claustre, M. Levy, D. A. Siegel, and T. Weber. 2019. Multi-faceted particle  
841 pumps drive carbon sequestration in the ocean. *Nature*. doi:10.1038/s41586-019-  
842 1098-2
- 843 Boyd, P. W., A. McDonnell, J. Valdez, D. LeFevre, and M. P. Gall. 2015. RESPIRE: An in  
844 situ particle interceptor to conduct particle remineralization and microbial dynamics  
845 studies in the oceans' Twilight Zone. *Limnology and Oceanography: Methods* **13**:  
846 494–508. doi:10.1002/lom3.10043
- 847 Briggs, N. T., W. H. Slade, E. Boss, and M. J. Perry. 2013. Method for estimating mean  
848 particle size from high-frequency fluctuations in beam attenuation or scattering  
849 measurements. *Appl. Opt., AO* **52**: 6710–6725. doi:10.1364/AO.52.006710
- 850 Burd, A. B., D. A. Hansell, D. K. Steinberg, and others. 2010. Assessing the apparent  
851 imbalance between geochemical and biochemical indicators of meso- and  
852 bathypelagic biological activity: What the @#! is wrong with present calculations of



- 853 carbon budgets? Deep-Sea Research Part II: Topical Studies in Oceanography  
854 1557–1571. doi:10.1016/j.dsr2.2010.02.022
- 855 Carlson, C. A., S. J. Giovannoni, D. A. Hansell, S. J. Goldberg, R. Parsons, and K. Vergin.  
856 2004. Interactions among dissolved organic carbon, microbial processes, and  
857 community structure in the mesopelagic zone of the northwestern Sargasso Sea.  
858 *Limnol. Oceanogr.* **49**: 1073–1083. doi:10.4319/lo.2004.49.4.1073
- 859 Chang, K. J. L., C. M. Nichols, S. I. Blackburn, G. A. Dunstan, A. Koutoulis, and P. D.  
860 Nichols. 2014. Comparison of *Thraustochytrids Aurantiochytrium* sp., *Schizochytrium*  
861 sp., *Thraustochytrium* sp., and *Ulkenia* sp. for Production of Biodiesel, Long-Chain  
862 Omega-3 Oils, and Exopolysaccharide. *Mar Biotechnol* 16.
- 863 Cho, B. C., and F. Azam. 1988. Major role of bacteria in biogeochemical fluxes in the  
864 ocean's interior. *Nature* **332**: 441–443. doi:10.1038/332441a0
- 865 Cole, H., S. Henson, A. Martin, and A. Yool. 2012. Mind the gap: The impact of missing data  
866 on the calculation of phytoplankton phenology metrics. *Journal of Geophysical*  
867 *Research: Oceans* **117**. doi:10.1029/2012JC008249
- 868 Collins, J. R., B. R. Edwards, K. Thamtrakoln, J. E. Ossolinski, G. R. DiTullio, K. D. Bidle,  
869 S. C. Doney, and B. A. S. Van Mooy. 2015. The multiple fates of sinking particles in  
870 the North Atlantic Ocean. *Global Biogeochemical Cycles* **29**: 1471–1494.  
871 doi:10.1002/2014GB005037
- 872 Cowen, J. P., M. A. Bertram, S. G. Wakeham, R. E. Thomson, J. William Lavelle, E. T.  
873 Baker, and R. A. Feely. 2001. Ascending and descending particle flux from  
874 hydrothermal plumes at Endeavour Segment, Juan de Fuca Ridge. *Deep Sea*  
875 *Research Part I: Oceanographic Research Papers* **48**: 1093–1120.  
876 doi:10.1016/S0967-0637(00)00070-4
- 877 Dong, S., A. V. Subhas, N. E. Rollins, J. D. Naviaux, J. F. Adkins, and W. M. Berelson. 2018.  
878 A kinetic pressure effect on calcite dissolution in seawater. *Geochimica et*  
879 *Cosmochimica Acta* **238**: 411–423. doi:10.1016/j.gca.2018.07.015



- 880 Edgcomb, V. P., C. Taylor, M. G. Pachiadaki, S. Honjo, I. Engstrom, and M. Yakimov. 2016.  
881 Comparison of Niskin vs. in situ approaches for analysis of gene expression in deep  
882 Mediterranean Sea water samples. *Deep Sea Research Part II: Topical Studies in*  
883 *Oceanography* **129**: 213–222. doi:10.1016/j.dsr2.2014.10.020
- 884 Eppley, R. W., and B. J. Peterson. 1979. Particulate organic matter flux and planktonic new  
885 production in the deep ocean. *Nature* **282**: 677–680. doi:10.1038/282677a0
- 886 Fennel, K., J. P. Mattern, S. C. Doney, L. Bopp, A. M. Moore, B. Wang, and L. Yu. 2022.  
887 Ocean biogeochemical modelling. *Nat Rev Methods Primers* **2**: 1–21.  
888 doi:10.1038/s43586-022-00154-2
- 889 Fuchs, R., C. M. J. Baumas, M. Garel, D. Nerini, F. A. C. Le Moigne, and C. Tamburini.  
890 2022. A RUpture-Based detection method for the Active mesopeLaglc Zone  
891 (RUBALIZ): A crucial step toward rigorous carbon budget assessments. *Limnology*  
892 *and Oceanography: Methods* **n/a**. doi:10.1002/lom3.10520
- 893 Fuhrman, J. 2000. Impact of Viruses on Bacterial Processes, *In* *Microbial ecology of the*  
894 *oceans*. Wiley.
- 895 Garel, M., P. Bonin, S. Martini, S. Guasco, M. Roumagnac, N. Bhairy, F. Armougom, and C.  
896 Tamburini. 2019. Pressure-Retaining Sampler and High-Pressure Systems to Study  
897 Deep-Sea Microbes Under In Situ Conditions. *Frontiers in Microbiology* **10**: 453.  
898 doi:10.3389/FMICB.2019.00453
- 899 Giering, S. L. C., E. L. Cavan, S. L. Basedow, and others. 2020. Sinking Organic Particles in  
900 the Ocean—Flux Estimates From in situ Optical Devices. *Frontiers in Marine Science*  
901 **6**. doi:10.3389/fmars.2019.00834
- 902 Giering, S. L. C., and C. Evans. 2022. Overestimation of prokaryotic production by leucine  
903 incorporation—and how to avoid it. *Limnology and Oceanography* 1–13.  
904 doi:10.1002/lno.12032
- 905 Giering, S. L. C., R. Sanders, R. S. Lampitt, and others. 2014. Reconciliation of the carbon  
906 budget in the ocean’s twilight zone. *Nature* **507**: 480–483. doi:10.1038/nature13123



- 907 Giering, S. L. C., R. Sanders, A. P. Martin, S. A. Henson, J. S. Riley, C. M. Marsay, and D.  
908 G. Johns. 2017. Particle flux in the oceans: Challenging the steady state assumption.  
909 Global Biogeochemical Cycles **31**. doi:10.1002/2016GB005424
- 910 del Giorgio, P. A., and J. J. Cole. 1998. BACTERIAL GROWTH EFFICIENCY IN NATURAL  
911 AQUATIC SYSTEMS. Annual Review of Ecology and Systematics **29**: 503–541.  
912 doi:10.1146/annurev.ecolsys.29.1.503
- 913 Grossart, H. P., and G. Gust. 2009. Hydrostatic pressure affects physiology and community  
914 structure of marine bacteria during settling to 4000 m: An experimental approach.  
915 Marine Ecology Progress Series **390**: 97–104. doi:10.3354/meps08201
- 916 Grossart, H.-P., and H. Ploug. 2000. Bacterial production and growth efficiencies: Direct  
917 measurements on riverine aggregates. Limnology and Oceanography **45**: 436–445.  
918 doi:10.4319/lo.2000.45.2.0436
- 919 Grossart, H.-P., and H. Ploug. 2001. Microbial degradation of organic carbon and nitrogen  
920 on diatom aggregates. Limnol. Oceanogr. **46**: 267–277.  
921 doi:10.4319/lo.2001.46.2.0267
- 922 Guieu, C., K. Desboeufs, S. Albani, and others. 2020. BIOGEOCHEMICAL dataset collected  
923 during the PEACETIME cruise. doi:https://doi.org/10.17882/75747
- 924 Hamamoto, Y., and D. Honda. 2019. Nutritional intake of Aplanochytrium (Labyrinthulea,  
925 Stramenopiles) from living diatoms revealed by culture experiments suggesting the  
926 new prey–predator interactions in the grazing food web of the marine ecosystem A.  
927 Ianora [ed.]. PLoS ONE **14**: e0208941. doi:10.1371/journal.pone.0208941
- 928 Henson, S. A., R. Sanders, E. Madsen, P. J. Morris, F. Le Moigne, and G. D. Quartly. 2011.  
929 A reduced estimate of the strength of the ocean’s biological carbon pump.  
930 Geophysical Research Letters **38**: n/a-n/a. doi:10.1029/2011GL046735
- 931 Herndl, G. J., T. Reinthaler, E. Teira, H. van Aken, C. Veth, A. Pernthaler, and J. Pernthaler.  
932 2005. Contribution of *Archaea* to Total Prokaryotic Production in the Deep Atlantic  
933 Ocean. Appl Environ Microbiol **71**: 2303–2309. doi:10.1128/AEM.71.5.2303-  
934 2309.2005



- 935 Herndl, G., and T. Reinthaler. 2013. Microbial control of the dark end of the biological pump.  
936 Nature Geoscience **6**: 718–724. doi:10.1038/ngeo1921
- 937 Homma, T., and A. Saltelli. 1996. Importance measures in global sensitivity analysis of  
938 nonlinear models. Reliability Engineering & System Safety **52**: 1–17.  
939 doi:10.1016/0951-8320(96)00002-6
- 940 Hoppe, H., and S. Ullrich. 1999. Profiles of ectoenzymes in the Indian Ocean: phenomena of  
941 phosphatase activity in the mesopelagic zone. Aquat. Microb. Ecol. **19**: 139–148.  
942 doi:10.3354/ame019139
- 943 Iversen, M. H., N. Nowald, H. Ploug, G. A. Jackson, and G. Fischer. 2010. High resolution  
944 profiles of vertical particulate organic matter export off Cape Blanc, Mauritania:  
945 Degradation processes and ballasting effects. Deep Sea Research Part I:  
946 Oceanographic Research Papers **57**: 771–784. doi:10.1016/j.dsr.2010.03.007
- 947 Jain, R., S. Raghukumar, R. Tharanathan, and N. B. Bhosle. 2005. Extracellular  
948 Polysaccharide Production by Thraustochytrid Protists. Mar Biotechnol **7**: 184–192.  
949 doi:10.1007/s10126-004-4025-x
- 950 Jannasch, H. W., and C. D. Taylor. 1984. Deep-Sea Microbiology. Annual Review of  
951 Microbiology **38**: 487–487. doi:10.1146/annurev.mi.38.100184.002415
- 952 de Jesus Mendes, P. A., L. Thomsen, B. Holscher, H. C. de Stigter, and G. Gust. 2007.  
953 Pressure effects on the biological degradation of organo-mineral aggregates in  
954 submarine canyons. Marine Geology **246**: 165–175.  
955 doi:10.1016/j.margeo.2007.05.012
- 956 Kjørboe, T. 2003. Marine snow microbial communities: scaling of abundances with  
957 aggregate size. Aquatic Microbial Ecology **33**: 67–75. doi:10.3354/ame033067
- 958 Kjørboe, T., H.-P. Grossart, H. Ploug, and K. Tang. 2002. Mechanisms and Rates of  
959 Bacterial Colonization of Sinking Aggregates. Applied and Environmental  
960 Microbiology **68**: 3996–4006. doi:10.1128/AEM.68.8.3996-4006.2002
- 961 Kjørboe, T., K. Tang, H.-P. Grossart, and H. Ploug. 2003. Dynamics of Microbial  
962 Communities on Marine Snow Aggregates: Colonization, Growth, Detachment, and





- 963            Grazing Mortality of Attached Bacteria. *Applied and Environmental Microbiology* **69**:  
964            3036–3047. doi:10.1128/AEM.69.6.3036-3047.2003
- 965    Kirchman, D., E. K'nees, and R. Hodson. 1985. Leucine incorporation and its potential as a  
966            measure of protein synthesis by bacteria in natural aquatic systems. *Applied and*  
967            *Environmental Microbiology* **49**: 599–607. doi:10.1128/aem.49.3.599-607.1985
- 968    Kirchman, D. L., and H. W. Ducklow. 1993. Estimating Conversion Factors for the Thymidine  
969            and Leucine Methods for Measuring Bacterial Production, *In Handbook of Methods in*  
970            *Aquatic Microbial Ecology*. Lewis publishers.
- 971    Koski, M., B. Valencia, R. Newstead, and C. Thiele. 2020. The missing piece of the upper  
972            mesopelagic carbon budget? Biomass, vertical distribution and feeding of aggregate-  
973            associated copepods at the PAP site. *Progress in Oceanography* **181**: 102243.  
974            doi:10.1016/j.pocean.2019.102243
- 975    Kuhlisch, C., G. Schleyer, N. Shahaf, F. Vincent, D. Schatz, and A. Vardi. 2021. Viral  
976            infection of algal blooms leaves a unique metabolic footprint on the dissolved organic  
977            matter in the ocean. *Science Advances* **7**: eabf4680. doi:10.1126/sciadv.abf4680
- 978    Kwon, E. Y., F. Primeau, and J. L. Sarmiento. 2009. The impact of remineralization depth on  
979            the air–sea carbon balance. *Nature Geosci* **2**: 630–635. doi:10.1038/ngeo612
- 980    Lagarias, J. C., J. A. Reeds, M. H. Wright, and P. E. Wright. 1998. Convergence properties  
981            of the Nelder-Mead simplex method in low dimensions. *SIAM Journal on*  
982            *Optimization* **9**: 112–147. doi:10.1137/S1052623496303470
- 983    Lampitt, R. S., B. Boorman, L. Brown, and others. 2008. Particle export from the euphotic  
984            zone: Estimates using a novel drifting sediment trap, <sup>234</sup>Th and new production.  
985            *Deep Sea Research Part I: Oceanographic Research Papers* **55**: 1484–1502.  
986            doi:10.1016/j.dsr.2008.07.002
- 987    Lara, E., D. Vaqué, E. L. Sà, and others. 2017. Unveiling the role and life strategies of  
988            viruses from the surface to the dark ocean. *Sci. Adv.* **3**: e1602565.  
989            doi:10.1126/sciadv.1602565



- 990 Le Moigne, F. A. C. 2019. Pathways of organic carbon downward transport by the oceanic  
991 biological carbon pump. *Frontiers in Marine Sciences* **6**: 1–8.  
992 doi:10.3389/fmars.2019.00634
- 993 Le Moigne, F. A. C., S. A. Henson, E. Cavan, and others. 2016. What causes the inverse  
994 relationship between primary production and export efficiency in the Southern  
995 Ocean? *Geophysical Research Letters* **43**: 4457–4466. doi:10.1002/2016GL068480
- 996 Lemée, R., E. Rochelle-Newall, F. Van Wambeke, M. Pizay, P. Rinaldi, and J. Gattuso.  
997 2002. Seasonal variation of bacterial production, respiration and growth efficiency in  
998 the open NW Mediterranean Sea. *Aquatic Microbial Ecology* **29**: 227–237.  
999 doi:10.3354/ame029227
- 1000 Liu, Y., M. Zeng, Z. Xie, D. Ning, J. Zhou, X. Yu, R. Liu, and L. Zhang. 2022. Microbial  
1001 Community Structure and Ecological Networks during Simulation of Diatom Sinking.  
1002 1–20.
- 1003 Luo, E., A. O. Leu, J. M. Eppley, D. M. Karl, and E. F. DeLong. 2022. Diversity and origins of  
1004 bacterial and archaeal viruses on sinking particles reaching the abyssal ocean. *The*  
1005 *ISME Journal* 1–9. doi:10.1038/s41396-022-01202-1
- 1006 Marsay, C. M., R. J. Sanders, S. A. Henson, K. Pabortsava, E. P. Achterberg, and R. S.  
1007 Lampitt. 2015. Attenuation of sinking particulate organic carbon flux through the  
1008 mesopelagic ocean. *Proceedings of the National Academy of Sciences* **112**: 1089–  
1009 1094. doi:10.1073/pnas.1415311112
- 1010 Martin, J. H., G. A. Knauer, D. M. Karl, and W. W. Broenkow. 1987. VERTEX: carbon cycling  
1011 in the northeast Pacific. *Deep Sea Research Part A. Oceanographic Research*  
1012 *Papers* **34**: 267–285. doi:10.1016/0198-0149(87)90086-0
- 1013 McDonnell, A. M. P., P. J. Lam, C. H. Lamborg, and others. 2015. The oceanographic  
1014 toolbox for the collection of sinking and suspended marine particles. *Progress in*  
1015 *Oceanography* **133**: 17–31. doi:10.1016/j.pocean.2015.01.007



- 1016 Mendes, P. A. de J., and L. Thomsen. 2012. Effects of Ocean Acidification on the Ballast of  
1017 Surface Aggregates Sinking through the Twilight Zone. *PLOS ONE* **7**: e50865.  
1018 doi:10.1371/journal.pone.0050865
- 1019 Nagata, T., C. Tamburini, J. Aristegui, and others. 2010. Emerging concepts on microbial  
1020 processes in the bathypelagic ocean – ecology, biogeochemistry, and genomics.  
1021 *Deep Sea Research Part II: Topical Studies in Oceanography* **57**: 1519–1536.  
1022 doi:10.1016/j.dsr2.2010.02.019
- 1023 Nelder, J. A., and R. Mead. 1965. A Simplex Method for Function Minimization. *The*  
1024 *Computer Journal* **7**: 308–313. doi:10.1093/comjnl/7.4.308
- 1025 Pedrosa-Pàmies, R., M. H. Conte, J. C. Weber, and R. Johnson. 2019. Hurricanes Enhance  
1026 Labile Carbon Export to the Deep Ocean. *Geophysical Research Letters* **46**: 10484–  
1027 10494. doi:10.1029/2019GL083719
- 1028 Picheral, M., C. Catalano, D. Brousseau, and others. 2022. THE UNDERWATER VISION  
1029 PROFILER 6: AN IMAGING SENSOR OF PARTICLE SIZE SPECTRA AND PLANKTON, FOR  
1030 AUTONOMOUS AND CABLED PLATFORMS. *Limnology & Ocean Methods* **20**: 115–129.  
1031 doi:10.1002/lom3.10475
- 1032 Planquette, H., and R. M. Sherrell. 2012. Sampling for particulate trace element  
1033 determination using water sampling bottles: methodology and comparison to in situ  
1034 pumps. *Limnology and Oceanography: Methods* **10**: 367–388.  
1035 doi:10.4319/lom.2012.10.367
- 1036 Reinthaler, T., H. M. van Aken, and G. J. Herndl. 2010. Major contribution of autotrophy to  
1037 microbial carbon cycling in the deep North Atlantic's interior. *Deep Sea Research*  
1038 *Part II: Topical Studies in Oceanography* **57**: 1572–1580.  
1039 doi:10.1016/j.dsr2.2010.02.023
- 1040 Reinthaler, T., H. van Aken, C. Veth, J. Aristegui, C. Robinson, P. J. L. B. Williams, P.  
1041 Lebaron, and G. J. Herndl. 2006. Prokaryotic respiration and production in the meso-  
1042 and bathypelagic realm of the eastern and western North Atlantic basin. *Limnology*  
1043 *and Oceanography* **51**: 1262–1273. doi:10.4319/lo.2006.51.3.1262



- 1044 Riley, J. S., R. Sanders, C. Marsay, F. A. C. Le Moigne, E. P. Achterberg, and A. J. Poulton.  
1045 2012. The relative contribution of fast and slow sinking particles to ocean carbon  
1046 export. *Global Biogeochemical Cycles* **26**: 1–10. doi:10.1029/2011GB004085
- 1047 Riou, V., J. Para, M. Garel, and others. 2018. Biodegradation of *Emiliania huxleyi*  
1048 aggregates by a natural Mediterranean prokaryotic community under increasing  
1049 hydrostatic pressure. *Progress in Oceanography* **163**: 271–281.  
1050 doi:10.1016/j.pocean.2017.01.005
- 1051 Robert, A. 2012. Minéralisation in situ de la matière organique le long de la colonne d'eau :  
1052 application sur une station eulérienne. These de doctorat. Aix-Marseille.
- 1053 Russell, J. B., and G. M. Cook. 1995. Energetics of Bacterial Growth: Balance of Anabolic  
1054 and Catabolic Reactions. *MICROBIOL. REV.* **59**: 15.
- 1055 Saint-Béat, B., B. D. Fath, C. Aubry, and others. 2020. Contrasting pelagic ecosystem  
1056 functioning in eastern and western Baffin Bay revealed by trophic network modeling.  
1057 *Elementa: Science of the Anthropocene* **8**. doi:10.1525/elementa.397
- 1058 Saint-Béat, B., F. Maps, and M. Babin. 2018. Unraveling the intricate dynamics of planktonic  
1059 Arctic marine food webs. A sensitivity analysis of a well-documented food web  
1060 model. *Progress in Oceanography* **160**: 167–185. doi:10.1016/j.pocean.2018.01.003
- 1061 Sherry, N. D., P. W. Boyd, K. Sugimoto, and P. J. Harrison. 1999. Seasonal and spatial  
1062 patterns of heterotrophic bacterial production, respiration, and biomass in the  
1063 subarctic NE Pacific. *Deep Sea Research Part II: Topical Studies in Oceanography*  
1064 **46**: 2557–2578. doi:10.1016/S0967-0645(99)00076-4
- 1065 Siegel, D. A., K. O. Buesseler, M. J. Behrenfeld, and others. 2016. Prediction of the Export  
1066 and Fate of Global Ocean Net Primary Production: The EXPORTS Science Plan.  
1067 *Frontiers in Marine Science* **3**: 22. doi:10.3389/fmars.2016.00022
- 1068 Simon, M., and F. Azam. 1989. Protein content and protein synthesis rates of planktonic  
1069 marine bacteria. *Marine Ecology Progress Series*. doi:10.3354/meps051201



- 1070 Smith, D. C., M. Simon, A. L. Alldredge, and F. Azam. 1992. Intense hydrolytic enzyme  
1071 activity on marine aggregates and implications for rapid particle dissolution. *Nature*  
1072 **359**: 139–142. doi:10.1038/359139a0
- 1073 Smith, K. L., P. M. Williams, and E. R. M. Druffel. 1989. Upward fluxes of particulate organic  
1074 matter in the deep North Pacific. *Nature* **337**: 724–726. doi:10.1038/337724a0
- 1075 Sobol, M. 1993. *Sensitivity Estimates for Nonlinear Mathematical Models*. 8.
- 1076 Stange, P., L. T. Bach, F. a. C. Le Moigne, J. Taucher, T. Boxhammer, and U. Riebesell.  
1077 2017. Quantifying the time lag between organic matter production and export in the  
1078 surface ocean: Implications for estimates of export efficiency. *Geophysical Research*  
1079 *Letters* **44**: 268–276. doi:10.1002/2016GL070875
- 1080 Steinberg, D. K., B. A. S. Van Mooy, K. O. Buesseler, P. W. Boyd, T. Kobari, and D. M. Karl.  
1081 2008. Bacterial vs. zooplankton control of sinking particle flux in the ocean's twilight  
1082 zone. *Limnology and Oceanography* **53**: 1327–1338. doi:10.4319/lo.2008.53.4.1327
- 1083 Stief, P., M. Elvert, and R. N. Glud. 2021. Respiration by “marine snow” at high hydrostatic  
1084 pressure: Insights from continuous oxygen measurements in a rotating pressure  
1085 tank. *Limnol Oceanogr* **66**: 2797–2809. doi:10.1002/lno.11791
- 1086 Tamburini, C., M. Boutrif, M. Garel, R. R. Colwell, and J. D. Deming. 2013. Prokaryotic  
1087 responses to hydrostatic pressure in the ocean—a review. *Environmental*  
1088 *microbiology reports* **15**: 1262–1274.
- 1089 Tamburini, C., J. Garcin, and A. Bianchi. 2003. Role of deep-sea bacteria in organic matter  
1090 mineralization and adaptation to hydrostatic pressure conditions in the NW  
1091 Mediterranean Sea. *Aquatic Microbial Ecology* **32**: 209–218. doi:10.3354/ame032209
- 1092 Tamburini, C., J. Garcin, G. Grégori, K. Leblanc, P. Rimmelin, and D. L. Kirchman. 2006.  
1093 Pressure effects on surface Mediterranean prokaryotes and biogenic silica  
1094 dissolution during a diatom sinking experiment. *Aquatic Microbial Ecology* **43**: 267–  
1095 276. doi:10.3354/ame043267
- 1096 Tamburini, C., J. Garcin, M. Ragot, and A. Bianchi. 2002. Biopolymer hydrolysis and  
1097 bacterial production under ambient hydrostatic pressure through a 2000m water



- 1098 column in the NW Mediterranean. *Deep Sea Research Part II: Topical Studies in*  
1099 *Oceanography* **49**: 2109–2123. doi:10.1016/S0967-0645(02)00030-9
- 1100 Tamburini, C., M. Garel, A. Barani, and others. 2021. Increasing Hydrostatic Pressure  
1101 Impacts the Prokaryotic Diversity during *Emiliana huxleyi* Aggregates Degradation.  
1102 *Water* **13**: 2616. doi:10.3390/w13192616
- 1103 Tamburini, C., M. Goutx, C. Guigue, and others. 2009. Effects of hydrostatic pressure on  
1104 microbial alteration of sinking fecal pellets. *Deep Sea Research Part II: Topical*  
1105 *Studies in Oceanography* **56**: 1533–1546. doi:10.1016/j.dsr2.2008.12.035
- 1106 Tarantola, A. 2005. *Inverse Problem Theory and Methods for Model Parameter Estimation*,  
1107 Society for Industrial and Applied Mathematics.
- 1108 Tian, R. C., A. F. Ve, B. Klein, T. Packard, S. Roy, C. Savenko, and N. Silverberg. 2000.  
1109 Effects of pelagic food-web interactions and nutrient remineralization on the  
1110 biogeochemical cycling of carbon: a modeling approach. 26.
- 1111 Trull, T. W., S. G. Bray, K. O. Buesseler, C. H. Lamborg, S. Manganini, C. Moy, and J.  
1112 Valdes. 2008. In situ measurement of mesopelagic particle sinking rates and the  
1113 control of carbon transfer to the ocean interior during the Vertical Flux in the Global  
1114 Ocean (VERTIGO) voyages in the North Pacific. *Deep Sea Research Part II: Topical*  
1115 *Studies in Oceanography* **55**: 1684–1695. doi:10.1016/j.dsr2.2008.04.021
- 1116 Turley, C., and P. Mackie. 1994. Biogeochemical significance of attached and free-living  
1117 bacteria and the flux of particles in the NE Atlantic Ocean. *Marine Ecology Progress*  
1118 *Series* **115**: 191–203. doi:10.3354/meps115191
- 1119 Turner, J. T. 2015. Zooplankton fecal pellets, marine snow, phytodetritus and the ocean's  
1120 biological pump. *Progress in Oceanography* **130**: 205–248.  
1121 doi:10.1016/j.pocean.2014.08.005
- 1122 Vetter, Y. A., J. W. Deming, P. A. Jumars, and B. B. Krieger-Brockett. 1998. A Predictive  
1123 Model of Bacterial Foraging by Means of Freely Released Extracellular Enzymes.  
1124 *Microb Ecol* **36**: 75–92. doi:10.1007/s002489900095



- 1125 Wakeham, S. G., C. Lee, J. I. Hedges, P. J. Hernes, and M. J. Peterson. 1997. Molecular  
1126 indicators of diagenetic status in marine organic matter. *Geochimica et*  
1127 *Cosmochimica Acta* **61**: 5363–5369. doi:10.1016/S0016-7037(97)00312-8
- 1128 Weiss, M. S., U. Abele, J. Weckesser, W. Welte, E. Schiltz, and G. E. Schulz. 1991.  
1129 Molecular architecture and electrostatic properties of a bacterial porin. *Science* **254**:  
1130 1627–1630. doi:10.1126/science.1721242
- 1131 Welch, W. J., M. -j. Gething, A. R. Clarke, and others. 1993. Heat shock proteins functioning  
1132 as molecular chaperones: their roles in normal and stressed cells. *Philosophical*  
1133 *Transactions of the Royal Society of London. Series B: Biological Sciences* **339**:  
1134 327–333. doi:10.1098/rstb.1993.0031
- 1135 Westerhoff, H. V., K. J. Hellingwerf, and K. Van Dam. 1983. Thermodynamic efficiency of  
1136 microbial growth is low but optimal for maximal growth rate. *Proc. Natl. Acad. Sci.*  
1137 *U.S.A.* **80**: 305–309. doi:10.1073/pnas.80.1.305
- 1138 Wilhem, W., and C. A. Suttle. 1999. Viruses and Nutrient Cycles in the Sea. **49**: 8.
- 1139 Xie, N., M. Bai, L. Liu, and others. 2022. Patchy Blooms and Multifarious Ecotypes of  
1140 Labyrinthulomycetes Protists and Their Implication in Vertical Carbon Export in the  
1141 Pelagic Eastern Indian Ocean A.L. Dos Santos [ed.]. *Microbiol Spectr* **10**: e00144-22.  
1142 doi:10.1128/spectrum.00144-22
- 1143 Yayanos, A. A. 1986. Evolutional and ecological implications of the properties of deep-sea  
1144 barophilic bacteria. *Proc. Natl. Acad. Sci. U.S.A.* **83**: 9542–9546.  
1145 doi:10.1073/pnas.83.24.9542
- 1146 Young, H. L. 1968. Uptake and Incorporation of Exogenous Leucine in Bacterial Cells under  
1147 High Oxygen Tension. *Nature* **219**: 1068–1069. doi:10.1038/2191068a0
- 1148